Annular axisymmetric stagnation flow of a non-Newtonian fluid on a moving cylinder

By

ABDUL REHMAN

Department of Mathematics
Quaid-i-Azam University, Islamabad
PAKISTAN

2010

Annular axisymmetric stagnation flow of a non-Newtonian fluid on a moving cylinder

By

ABDUL REHMAN

Supervised

By

DR. SOHAIL NADEEM

Department of Mathematics
Quaid-i-Azam University, Islamabad
PAKISTAN

2010

Annular axisymmetric stagnation flow of a non-Newtonian fluid on a moving cylinder

By

Abdul Rehman

A Dissertation Submitted in the partial fulfillment of the requirements for the degree of

MASTER OF PHILOSOPHY

IN

MATHEMATICS

Supervised By

Dr. Sohail Nadeem

Department of Mathematics
Quaid-i-Azam University, Islamabad
PAKISTAN

2010

CERTIFICATE

Annular axisymmetric stagnation flow of a non-Newtonian fluid on a moving cylinder

By

Abdul Rehman

A DISSERTATION SUBMITTED IN THE PARTIAL FULFILLMENT OF THE REQUIREMENTS FOR THE DEGREE OF THE MASTER OF PHILOSOPHY

We accept this dissertation as conforming to the required standard

1. ______________________
Prof Dr. Muhammad Ayub
(Chairman)

2. ______________________
Dr. Sohail Nadeem
(Supervisor)

3. ______________________
Prof Dr. Saleem Asghar
(External Examiner)

Department of Mathematics
Quaid-i-Azam University, Islamabad

Acknowledgement

I am highly grateful to Almighty Allah for His blessing and help in each and every step of my life and especially for this work.

I would not have been able to complete my work with out the guidance of my supervisor, **Dr. Sohail Nadeem** who always treated me with care.

Chairman, Department of Mathematics, **Prof. Dr. Muhammad Ayub** should also be thanked for how smoothly he is running the Department.

I am also grateful to the Higher Education Commission (HEC) of Pakistan for its financial support as with out the assistance of HEC I may not have been able to complete my work.

Abdul Rehman

Preface

Numerous applications of stagnation flows in engineering and scientific interest have attracted the attention of number of researchers. Mention may be made to the interesting works of [1-10]. In some situations flow is stagnated by a solid wall, while in others a free stagnation point or line exist interior to the fluid domain [11]. The stagnation point flows can be viscous or inviscid, steady or unsteady, two dimensional or three dimensional, normal or oblique and forward or reverse. The stagnation flows were initiated by Hiemenz [12] and Homann [13]. Recently, Hong and Wang [14] have discussed the annular axisymmetric stagnation flow on a moving cylinder. According to them [14], in the previous literature the researchers have considered a stagnation flow originated from infinity. But there are certain situations in which finite geometry is more realistic and attractive for high speed and miniature rotating systems [15-16].

In the situations like polymeric fluids or certain naturally occurring fluids such as animal blood, the classical Navier Stokes theory does not hold [16]. Therefore, Erigen [17] has given the idea of micropolar fluid which describes both the effect of couple stresses and the microscopic effects arising from local structure and microrotation of the fluid elements. Also, the micropolar fluids consist of a suspension of small, rigid, cylindrical elements such as large dumbbell shaped molecules. Erigen [18] has also developed the theory of thermomicropolar fluids by extending the theory of micropolar fluids. Because of importance of this theory a large amount of literature on micropolar fluids with different geometries are now available. Few of them are cited in the Ref [19-25].

Motivated from the above highlights, the purpose of the present work is to extend the idea of Hong and Wang [14] for micropolar fluid. To the best of author's knowledge, not only a single article is available in literatures which discuss the axisymmetric stagnation flow of non-Newtonian fluid in a finite geometry. The problem has been first simplified with the help of suitable similarity transformations and then solved with the analytical technique known as homotopy analysis method (HAM), some relevant work on HAM are given in the Ref [26-36]. The convergence of the HAM solution has been discussed through h-curves. The thesis is arranged as follows:

In chapter one, the idea of Hong and Wang has been utilized and find analytical solution with the help of HAM. The comparison of numerical solutions [14] and our HAM solution is also presented. Chapter two is devoted to the study of stagnation flow of a micropolar fluid in a moving cylinder. After reducing the problem with the problem with the help of suitable similarity transformations the problem is solved analytically with the help of HAM. The convergence of the problem is discussed by plotting h-curves. At the end, the physical behaviors of pertinent parameters are discussed through graphs and tables.

Contents

Chapter 1

Annular axisymmetric stagnation flow on a moving cylinder

1.1 Introduction

In this chapter, we have discussed the axisymmetric stagnation flow of a viscous fluid in a moving cylinder. The governing equations of viscous fluid along with energy equations are modelled in cylindrical coordinates system. The coupled nonlinear equations are simplified with the help of suitable similarity transformations and then the reduced equations are solved analytically with the help of perturbation method and homotopy analysis method. Originally, this physical problem has been given by Hong and Wang [14], they have presented the perturbation and numerical solutions. We have solved this problem with the help of Homotopy analysis method (HAM) and the results are compared with the available numerical results. It is found that both the results are almost identical.

1.2 Mathematical formulation

We consider the stagnation point flow[1] of viscous fluid between two concentric cylinders. The outer cylinder is fixed while the inner cylinder is rotating about z-axis with constant angu-

[1] Stagnation point is a point in a flow field where the local velocity of the fluid is zero. Stagnation points exist at the surface of objects in the flow field, where the fluid is brought to rest by the object.

lar velocity Ω and having linear translation along z-axis. The governing equations of mass, momentum, and energy are

$$\operatorname{div} \mathbf{V} = 0, \tag{1.1}$$

$$\rho \frac{d\mathbf{V}}{dt} = \operatorname{div} \mathbf{T}, \tag{1.2}$$

$$\rho c_p \frac{d\sigma}{dt} = \mathbf{T}.\mathbf{L} - \operatorname{div} \mathbf{q}, \tag{1.3}$$

where $\mathbf{V}$ is the velocity vector, ρ is the density, $\mathbf{T}$ is the Cauchy stress tensor, c_p is the specific heat, σ is the temperature and $\mathbf{q}\,(= -k \operatorname{div} \sigma)$ is the heat flux[1].

The Cauchy stress tensor for viscous fluid is defined as

$$\mathbf{T} = -p\mathbf{I} + \mu \mathbf{A}_1 \tag{1.4}$$

in which p is the pressure, $\mathbf{I}$ is the unit tensor, μ is the viscosity and $\mathbf{A}_1$ is the first Rivlin Ericksen tensor which is defined as

$$\mathbf{A}_1 = (\operatorname{grad} \mathbf{V}) + (\operatorname{grad} \mathbf{V})^T. \tag{1.5}$$

We seek the velocity and temperature fields of the form

$$\mathbf{V} = [u(r,z), v(r,z), w(r,z)], \quad \sigma = \sigma(r,z). \tag{1.6}$$

With the help of $Eqs.\,(1.4)$ to (1.6), $Eqs.\,(1.1)$ to (1.3), take the following form

$$u_r + w_z + \frac{u}{r} = 0, \tag{1.7}$$

$$\rho\left[uu_r + wu_z - \frac{v^2}{r}\right] = -\frac{\partial p}{\partial r} + \mu\left(\frac{1}{r}\frac{\partial}{\partial r}(r\tau_{rr}) + \frac{\partial}{\partial z}(\tau_{zr}) - \frac{\tau_{\theta\theta}}{r}\right), \tag{1.8}$$

$$\rho\left[uv_r + wv_z + \frac{uv}{r}\right] = \mu\left(\frac{1}{r^2}\frac{\partial}{\partial r}(r^2\tau_{r\theta}) + \frac{\partial}{\partial z}(\tau_{z\theta}) + \frac{\tau_{\theta r} - \tau_{r\theta}}{r}\right), \tag{1.9}$$

$$\rho[uw_r + ww_z] = -\frac{\partial p}{\partial z} + \mu\left(\frac{1}{r}\frac{\partial}{\partial r}(r\tau_{rz}) + \frac{\partial}{\partial z}(\tau_{zz})\right), \tag{1.10}$$

[1] rate of flow of heat energy per unit area

$$\rho c_p\left[u\sigma_r + w\sigma_z\right] = \overrightarrow{\mathbf{T}}.\overrightarrow{\mathbf{L}} + k\left(\sigma_{rr} + \frac{1}{r}\sigma_r + \sigma_{zz}\right), \tag{1.11}$$

where

$$\begin{bmatrix} \tau_{rr} & \tau_{r\theta} & \tau_{rz} \\ \tau_{\theta r} & \tau_{\theta\theta} & \tau_{\theta z} \\ \tau_{zr} & \tau_{z\theta} & \tau_{zz} \end{bmatrix} = \begin{bmatrix} 2u_r & v_r - \frac{v}{r} & w_r + u_z \\ v_r - \frac{v}{r} & \frac{2u}{r} & v_z \\ w_r + u_z & v_z & w_z \end{bmatrix}. \tag{1.12}$$

With the help of $Eq.\,(1.12)$, $Eqs.\,(1.8)$ to (1.11) take the following form

$$\rho\left(uu_r + wu_z - \frac{v^2}{r}\right) = -\frac{\partial p}{\partial r} + \mu\left(u_{rr} + \frac{1}{r}u_r + u_{zz} - \frac{u}{r^2}\right), \tag{1.13}$$

$$\rho\left(uv_r + wv_z + \frac{uv}{r}\right) = \mu\left(v_{rr} + \frac{1}{r}v_r + v_{zz} - \frac{v}{r^2}\right), \tag{1.14}$$

$$\rho\left(uw_r + ww_z\right) = -\frac{\partial p}{\partial z} + \mu\left(w_{rr} + \frac{1}{r}w_r + w_{zz}\right), \tag{1.15}$$

$$\begin{aligned} \rho c_p\left(u\sigma_r + w\sigma_z\right) &= \mu(2u_r^2 + v_r^2 - \frac{2vv_r}{r} + 2u_z w_r + w_r^2 + \frac{v^2}{r^2} + \frac{2u^2}{r^2} \\ &\quad + u_z^2 + v_z^2 + 2w_z^2) + k\left(\sigma_{rr} + \frac{1}{r}\sigma_r + \sigma_{zz}\right). \end{aligned} \tag{1.16}$$

Elimination of pressure from $Eqs.\,(1.13)$ and (1.15) yields

$$\begin{aligned} &\rho\left(uu_{rz} + u_r u_z + wu_{zz} + u_z w_z - \frac{2vv_z}{r} - u_r w_r - uw_{rr} - w_r w_z - ww_{rz}\right) \\ = \;&\mu\left(u_{rrz} + \frac{1}{r}u_{rz} + u_{zzz} - \frac{u_z}{r^2} - w_{rrr} - \frac{1}{r}w_{rr} + \frac{1}{r^2}w_r - w_{rzz}\right). \end{aligned} \tag{1.17}$$

Making use of $Eq.\,(1.7)$, $Eq.\,(1.17)$ takes the following form

$$\begin{aligned} &uu_{rz} - \frac{u}{r}u_z + wu_{zz} - \frac{2vv_z}{r} + \frac{u}{r}w_r - uw_{rr} - ww_{rz} \\ = \;&\nu\left(u_{rrz} + \frac{1}{r}u_{rz} + u_{zzz} - \frac{u_z}{r^2} - w_{rrr} - \frac{1}{r}w_{rr} + \frac{1}{r^2}w_r - w_{rzz}\right). \end{aligned} \tag{1.18}$$

According to the geometry of the problem, the boundary conditions take the following form

$$\mathbf{V}(R,z) = (0, a\Omega, 0), \quad \mathbf{V}(bR,z) = (-U,0,0), \quad \sigma(R,z) = \sigma_1, \quad \sigma(bR,z) = \sigma_2. \tag{1.19}$$

Defining the following similarity transformations

$$
\begin{aligned}
u &= \frac{-Uf(\eta)}{\eta}, \quad v = a\Omega h(\eta), \quad w = 2Uf'(\eta)\xi + Wg(\eta), \quad \theta = \frac{\sigma - \sigma_1}{\sigma_2 - \sigma_1}, \\
\eta &= \frac{r^2}{R^2}, \quad \xi = \frac{z}{R}.
\end{aligned} \tag{1.20}
$$

With the help of $Eq.(1.20)$, $Eqs.(1.18)$, (1.14) and (1.16) take the following form

$$
\begin{aligned}
& \frac{RU}{2\nu}\left[-f\left(2Uf'''\xi + Wg''\right) + f''\left(2Uf'\xi + Wg\right)\right] \\
= \ & \eta\left(2Uf^{iv}\xi + Wg'''\right) + 2\left(2Uf'''\xi + Wg''\right) \\
& -\frac{R^2\sigma B_0^2}{4\nu\rho}\left(2Uf''\xi + Wg'\right),
\end{aligned} \tag{1.21}
$$

$$4\eta h'' + 4h' - \frac{h}{\eta} + \mathrm{Re}\left(4fh' + \frac{2fh}{\eta}\right) = 0, \tag{1.22}$$

$$\eta\theta'' + \theta' + \mathrm{Pr}\,\mathrm{Re}\, f\theta' = 0, \tag{1.23}$$

where $\mathrm{Pr} = \frac{\nu\rho c_p}{k^*}$ is the Prandtl number.

Equating the coefficients of like powers of ξ in $Eq.(1.21)$, we have

$$\eta f^{iv} + 2f''' + \mathrm{Re}\left(ff''' - f'f''\right) = 0, \tag{1.24}$$

$$\mathrm{Re}\left(f'g - fg'\right)' = (\eta g'')' + (g')'. \tag{1.25}$$

Integration of $Eq.(1.25)$, gives

$$\eta g'' + g' + \mathrm{Re}\left(fg' - f'g\right) = 0, \tag{1.26}$$

where $\mathrm{Re} = \frac{RU}{2v}$ is the Reynolds's number.

The corresponding boundary conditions take the following form

$$
\begin{aligned}
f(1) &= 0, \quad f'(1) = 0, \quad g(1) = 1, \quad h(1) = 1, \\
f(b) &= \sqrt{b}, \quad f'(b) = 0, \quad g(b) = 0, \quad h(b) = 0.
\end{aligned} \tag{1.27}
$$

$Eqs.$ (1.22) to (1.24) and (1.26) are highly nonlinear coupled equations, their exact solutions are impossible, therefore we want to solve it analytically with the help of perturbation method and homotopy analysis method.

1.3 Solution of the problem

1.3.1 Perturbation solution for small Reynolds numbers

Since Reynolds number is defined as $\mathrm{Re} = \frac{RU}{2\upsilon}$, we assume that $\mathrm{Re} << 1$, that is either the injection velocity, or the diameter of the inner cylinder is small, or the viscosity of the fluid is large, we expand the solution in terms of the Reynolds numbers as

$$
\begin{aligned}
f &= f_0 + \mathrm{Re}\, f_1 + \cdots, && (1.28)\\
g &= g_0 + \mathrm{Re}\, g_1 + \cdots, && (1.29)\\
h &= h_0 + \mathrm{Re}\, h_1 + \cdots. && (1.30)
\end{aligned}
$$

Substituting $Eqs.$ (1.28) to (1.30) into $Eqs.$ (1.22), (1.24) and (1.26), we obtain the following systems

Zeroth order system

$$
\begin{aligned}
\eta f_0^{iv} + 2f_0''' &= 0, && (1.31)\\
\eta g_0'' + g_0' &= 0, && (1.32)\\
4\eta h_0'' + 4h_0' - \frac{h_0}{\eta} &= 0. && (1.33)
\end{aligned}
$$

With the boundary conditions

$$
\begin{aligned}
f_0(1) &= 0,\ f_0'(1) = 0,\ g_0(1) = 1,\ h_0(1) = 1,\\
f_0(b) &= \sqrt{b},\ f_0'(b) = 0,\ g_0(b) = 0,\ h_0(b) = 0. && (1.34)
\end{aligned}
$$

First order system

$$\eta f_1^{iv} + 2f_1''' = f_0 f_0''' - f_0' f_0'', \tag{1.35}$$

$$\eta g_1'' + g_1' = f_0' g_0 - f_0 g_0', \tag{1.36}$$

$$4\eta h_1'' + 4h_1' - \frac{h_1}{\eta} = -4f_0 h_0' - \frac{2f_0 h_0}{\eta}. \tag{1.37}$$

The related boundary conditions at this order are defined as

$$f_1(1) = 0,\ f_1'(1) = 0,\ g_1(1) = 0,\ h_1(1) = 0, \tag{1.38}$$

$$f_1(b) = 0,\ f_1'(b) = 0,\ g_1(b) = 0,\ h_1(b) = 0. \tag{1.39}$$

Solution of zeroth order system

The solution of $Eqs.$ (1.31).to (1.33) , satisfying the boundary condition (1.34) take the following form

$$f_0 = \frac{\sqrt{b}\left[-2(b-1)\eta Ln[\eta] + Ln[b]\eta^2 + 2(b-1-Ln[b])\eta - (2b-2-Ln[b])\right]}{(b-1)\left[2(b-1)-(b+1)Ln[b]\right]}, \tag{1.40}$$

$$g_0 = \frac{Ln[b] - Ln[\eta]}{Ln[b]}, \qquad h_0 = \frac{\eta - b}{(1-b)\sqrt{\eta}}. \tag{1.41}$$

Solution of first order system

With the help of zeroth order solution the solution of first order system is computed and is shown through graph as follows

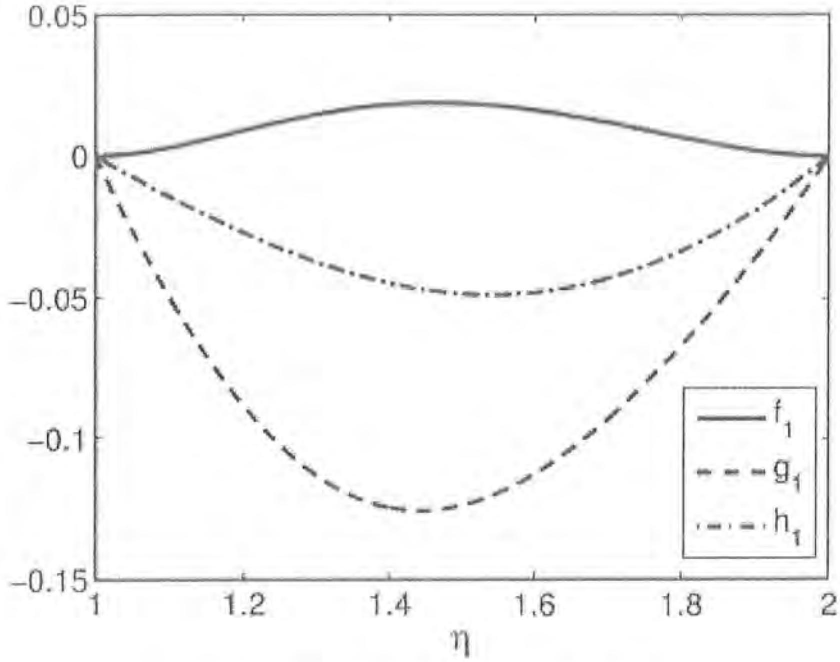

*Fig*1.1, variation of velocity against η

The expressions for different boundary derivatives are defined as

$$f''(1) = \frac{2\sqrt{b}\,[Ln[b]-(b+1)]}{(b-1)\,[2\,(b-1)-(b+1)\,Ln[b]]} + \operatorname{Re} f_1''(1) + O(\operatorname{Re}^2), \tag{1.42}$$

$$f'''(1) = \frac{2\sqrt{b}}{2\,(b-1)-(b+1)\,Ln[b]} + \operatorname{Re} f_1''(1) + O(\operatorname{Re}^2), \tag{1.43}$$

$$g'(1) = -\frac{1}{Ln[b]} + \operatorname{Re} g_1'(1) + O(\operatorname{Re}^2), \tag{1.44}$$

$$h'(1) = -\frac{b+1}{2\,(b-1)} + \operatorname{Re} h_1'(1) + O(\operatorname{Re}^2), \tag{1.45}$$

1.3.2 Perturbation solution for small gap width

When the annular gap width (*say* ϵ) is small, that is $\epsilon << 1$, we can set $\eta = 1 + \epsilon\sigma$, for $0 < \sigma < 1$, expanding in terms of ϵ we have

$$f(\eta) = \Phi_0(\sigma) + \epsilon\Phi_1(\sigma) + \cdots, \tag{1.46}$$

$$g(\eta) = \Psi_0(\sigma) + \epsilon\Psi_1(\sigma) + \cdots, \tag{1.47}$$

$$h(\eta) = \Lambda_0(\sigma) + \epsilon\Lambda_1(\sigma) + \cdots. \tag{1.48}$$

With the help of *Eqs.* (1.46) to (1.48) into *Eqs.* (1.22), (1.24) and (1.26), using the similar procedure as discussed in previous section, the solutions are straightforward defined as

$$\Phi_1(\sigma) = \frac{5}{2}\sigma^2 - 3\sigma^3 + \sigma^4 + \mathrm{Re}\left(\frac{8}{35}\sigma^2 - \frac{27}{70}\sigma^3 + \frac{3}{10}\sigma^5 - \frac{1}{5}\sigma^6 + \frac{2}{35}\sigma^7\right), \tag{1.49}$$

$$\Psi_1(\sigma) = -\frac{1}{2}\sigma + \frac{1}{2}\sigma^2 + \mathrm{Re}\left(-\frac{9}{20}\sigma + \sigma^3 - \frac{3}{4}\sigma^4 + \frac{1}{5}\sigma^5\right), \tag{1.50}$$

$$\Lambda_1(\sigma) = -\frac{1}{2}\sigma + \frac{1}{2}\sigma^2 + \mathrm{Re}\left(-\frac{3}{20}\sigma + \frac{1}{4}\sigma^4 - \frac{1}{10}\sigma^5\right). \tag{1.51}$$

The boundary derivatives are

$$f''(1) = \frac{1}{\epsilon^2}[6 + \epsilon\left(5 + \frac{16}{35}\mathrm{Re}\right) + \cdots], \tag{1.52}$$

$$f'''(1) = \frac{1}{\epsilon^2}[-12 - \epsilon\left(18 + \frac{81}{35}\mathrm{Re}\right) + \cdots], \tag{1.53}$$

$$g'(1) = \frac{1}{\epsilon}[-1 - \epsilon\left(\frac{1}{2} + \frac{9}{20}\mathrm{Re}\right) + \cdots], \tag{1.54}$$

$$h'(1) = \frac{1}{\epsilon}[-1 - \epsilon\left(\frac{1}{2} + \frac{3}{20}\mathrm{Re}\right) + \cdots]. \tag{1.55}$$

1.3.3 Solution by Homotopy analysis method

In this section, the solution of the above boundary value problem is obtained with the help of HAM. For HAM solution we choose the initial guesses as [26-36]

$$f_0(\eta) = \frac{\sqrt{b}}{b-1}((3b-1) - 6b\eta + 3(b+1)\eta^2 - 2\eta^3), \tag{1.56}$$

$$g_0(\eta) = \frac{b-\eta}{b-1}, \quad h_0(\eta) = \frac{b-\eta}{b-1}, \quad \theta_0(\eta) = \frac{\eta-1}{b-1}, \tag{1.57}$$

the corresponding auxiliary linear operators are

$$L_f = \frac{d^4}{d\eta^4}, \quad L_g = \frac{d^2}{d\eta^2}, \quad L_h = \frac{d^2}{d\eta^2}, \quad L_\theta = \frac{d^2}{d\eta^2}, \tag{1.58}$$

which satisfy

$$L_f[c_1 + c_2\eta + c_3\eta^2 + c_4\eta^3] = 0, \tag{1.59}$$

$$L_g[c_5 + c_6\eta] = 0, \quad L_h[c_7 + c_8\eta] = 0, \quad L_\theta[c_9 + c_{10}\eta] = 0, \tag{1.60}$$

where c_i $(i = 1, ..., 10)$ are arbitrary constants while the zeroth-order deformation equations are defined as

$$(1-p) L_f[\hat{f}(\eta;p) - f_0(\eta)] = p\hbar_1 N_f[\hat{f}(\eta;p)], \tag{1.61}$$

$$(1-p) L_g[\hat{g}(\eta;p) - g_0(\eta)] = p\hbar_2 N_g[\hat{g}(\eta;p)], \tag{1.62}$$

$$(1-p) L_h[\hat{h}(\eta;p) - h_0(\eta)] = p\hbar_3 N_h[\hat{h}(\eta;p)], \tag{1.63}$$

$$(1-p) L_\theta[\hat{\theta}(\eta;p) - \theta_0(\eta)] = p\hbar_4 N_\theta[\hat{\theta}(\eta;p)], \tag{1.64}$$

in which

$$N_f[\hat{f}(\eta;p)] = \eta\hat{f}^{iv} + 2\hat{f}''' + \mathrm{Re}(\hat{f}\hat{f}''' - \hat{f}'\hat{f}''), \tag{1.65}$$

$$N_g[\hat{g}(\eta;p)] = \eta\hat{g}'' + \hat{g}' + \mathrm{Re}(\hat{f}\hat{g}' - \hat{f}'\hat{g}), \tag{1.66}$$

$$N_h[\hat{h}(\eta;p)] = 4\eta^2\hat{h}'' + 4\eta\hat{h}' - \hat{h} + \mathrm{Re}(4\eta\hat{f}\hat{h}' + 2\hat{f}\hat{h}), \tag{1.67}$$

$$N_\theta[\hat{\theta}(\eta;p)] = \eta\hat{\theta}'' + \hat{\theta}' + \mathrm{Pr}\,\mathrm{Re}\,\hat{f}\hat{\theta}'. \tag{1.68}$$

The boundary conditions for the zeroth order system are defined as

$$\hat{f}\,(1;p)=0,\;\hat{f}'(1;p)=0,\;\hat{g}\,(1;p)=1,\;\hat{h}\,(1;p)=1,\;\hat{\theta}\,(1;p)=0, \tag{1.69}$$

$$\hat{f}\,(b;p)=\sqrt{b},\;\hat{f}'\,(b;p)=0,\;\hat{g}\,(b;p)=0,\;\hat{h}\,(b;p)=0,\;\hat{\theta}\,(b;p)=1. \tag{1.70}$$

The mth order deformation equations can be obtained by differentiating the zeroth-order deformation $Eqs.\,(1.61-1.64)$ and the boundary conditions $(1.69-1.70)$, m-times with respect to p, then dividing by $m!$ and finally setting $p=0$, we obtain

$$L_f[f_m\,(\eta)-\chi_m f_{m-1}\,(\eta)]=\hbar_1 R_{mf}\,(\eta)\,, \tag{1.71}$$

$$L_g[g_m\,(\eta)-\chi_m g_{m-1}\,(\eta)]=\hbar_2 R_{mg}\,(\eta)\,, \tag{1.72}$$

$$L_h[h_m\,(\eta)-\chi_m h_{m-1}\,(\eta)]=\hbar_3 R_{mh}\,(\eta)\,, \tag{1.73}$$

$$L_\theta[\theta_m\,(\eta)-\chi_m \theta_{m-1}\,(\eta)]=\hbar_4 R_{m\theta}\,(\eta)\,, \tag{1.74}$$

$$f_m\,(1)=0,\quad f_m'\,(1)=0,\quad g_m\,(1)=0,\quad h_m\,(1)=0,\quad \theta_m\,(1)=0, \tag{1.75}$$

$$f_m\,(b)=0,\quad f_m'\,(b)=0,\quad g_m\,(b)=0,\quad h_m\,(b)=0,\quad \theta_m\,(b)=0, \tag{1.76}$$

where

$$R_{mf}\,(\eta)=\eta f_{m-1}^{''''}+2f_{m-1}^{'''}+\mathrm{Re}\sum_{j=0}^{m}(f_j f_{m-1-j}^{'''}-f_j^{'}f_{m-1-j}^{''}), \tag{1.77}$$

$$R_{mg}\,(\eta)=\eta g_{m-1}^{''}+g_{m-1}^{'}+\mathrm{Re}\sum_{j=0}^{m}(f_j g_{m-1-j}^{'}-f_j^{'}g_{m-1-j}), \tag{1.78}$$

$$R_{mh}\,(\eta)=4\eta^2 h_{m-1}^{''}+4\eta h_{m-1}^{'}-h_{m-1}+\mathrm{Re}\sum_{j=0}^{m}(4\eta f_j h_{m-1-j}^{'}+2f_j h_{m-1-j}), \tag{1.79}$$

$$R_{m\theta}\,(\eta)=\eta\theta_{m-1}^{''}+\theta_{m-1}^{'}+\Pr\mathrm{Re}\sum_{j=0}^{m}f_j\theta_{m-1-j}^{'}, \tag{1.80}$$

$$\chi_m=\begin{cases}0 & m\leq 1\\ 1 & m>1.\end{cases} \tag{1.81}$$

With the help of software MATHEMATICA, the solutions of *Eqs.* (1.22) to (1.24) and (1.26) subject to the boundary conditions (1.27) can be defined as

$$f(\eta) = \lim_{Q\to\infty} [\sum_{m=1}^{Q} f_m(\eta)], \quad g(\eta) = \lim_{Q\to\infty} [\sum_{m=1}^{Q} g_m(\eta)], \tag{1.82}$$

$$h(\eta) = \lim_{Q\to\infty} [\sum_{m=1}^{Q} h_m(\eta)], \quad \theta(\eta) = \lim_{Q\to\infty} [\sum_{m=1}^{Q} \theta_m(\eta)], \tag{1.83}$$

where

$$f_m(\eta) = f_m^*(\eta) + C_1 + C_2\eta + C_3\eta^2 + C_4\eta^3, \tag{1.84}$$

$$g_m(\eta) = g_m^*(\eta) + C_5 + C_6\eta, \tag{1.85}$$

$$h_m(\eta) = h_m^*(\eta) + C_7 + C_8\eta, \tag{1.86}$$

$$\theta_m(\eta) = \theta_m^*(\eta) + C_9 + C_{10}\eta, \tag{1.87}$$

In above equations $f_m^*(\eta), g_m^*(\eta), h_m^*(\eta)$ and $\theta_m^*(\eta)$ are the special solutions and can be stated as

$$f_m^*(\eta) = \sum_{n=1}^{\infty} a_{mn}\eta^{4n+3}, \quad g_m^*(\eta) = \sum_{n=1}^{\infty} b_{mn}\eta^{4n+1}, \tag{1.88}$$

$$h_m^*(\eta) = \sum_{n=1}^{\infty} c_{mn}\eta^{5n+1}, \quad \theta_m^*(\eta) = \sum_{n=1}^{\infty} d_{mn}\eta^{4n+1}. \tag{1.89}$$

1.4 Results and discussion

In this section, we have discussed the perturbation solution and HAM solution through graphs and tables. In *Fig.*1.1, first order perturbation solutions have been plotted against η. It is seen that f_1 gives maximum value and h_1 gives minimum value. The h-curves for f, g, h and θ are plotted in *Fig.*1.2 to 1.6. The related convergence regions are $-1 < h < -0.3$, $-1 < h < -0.4$, $-0.125 < h < -0.1$, $-1 < h < -0.6$ and $-0.9 < h < -0.65$ for f, g, h and θ respectively. The variation of Re on f, g, h and θ are displayed in *Fig.*1.7 to 1.10. It is seen that with the increase in Re, f and θ increases while g and h decreases. The variation of Pr on θ are shown in *Fig.*1.11. It is observed that temperature profile increases with the increase in Pr.

A comparison of numerical, perturbation and HAM solutions are given in tables 1.1 to 1.12

for different functions. It is seen that the numerical and HAM solutions are in good agreement with each other.

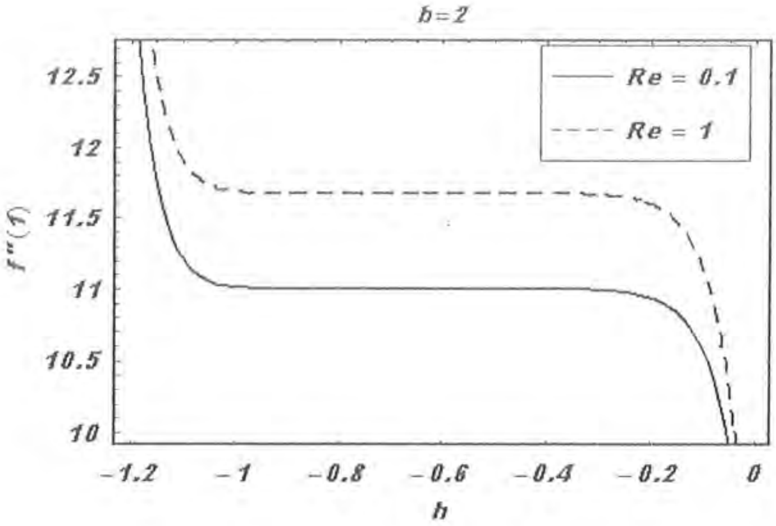

*Fig.*1.2. h-curves for f against different Re.

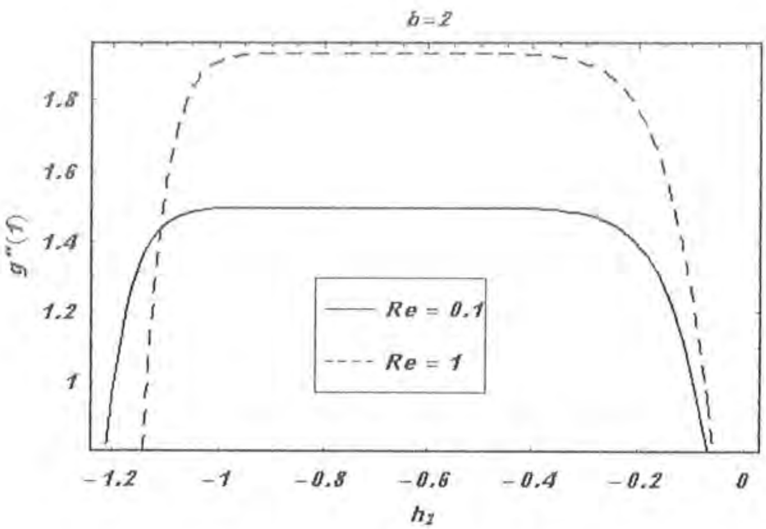

*Fig.*1.3. h-curves for g against different Re.

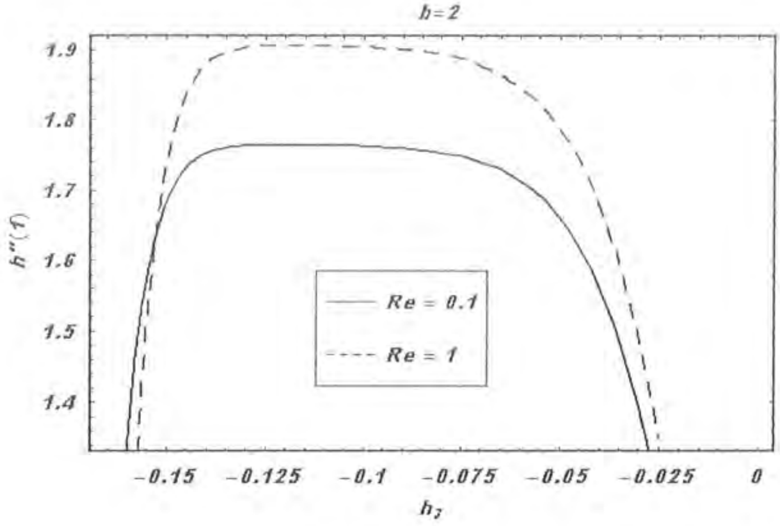

Fig.1.4. h-curves for h against different Re.

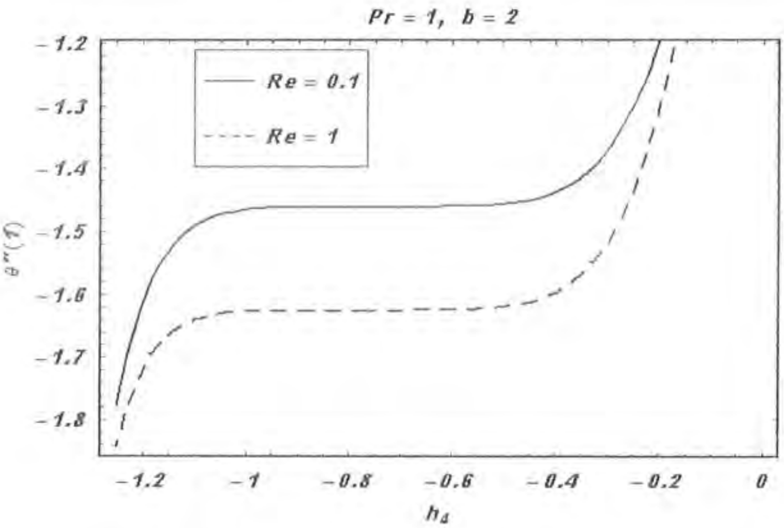

Fig.1.5. h-curves for θ against different Re.

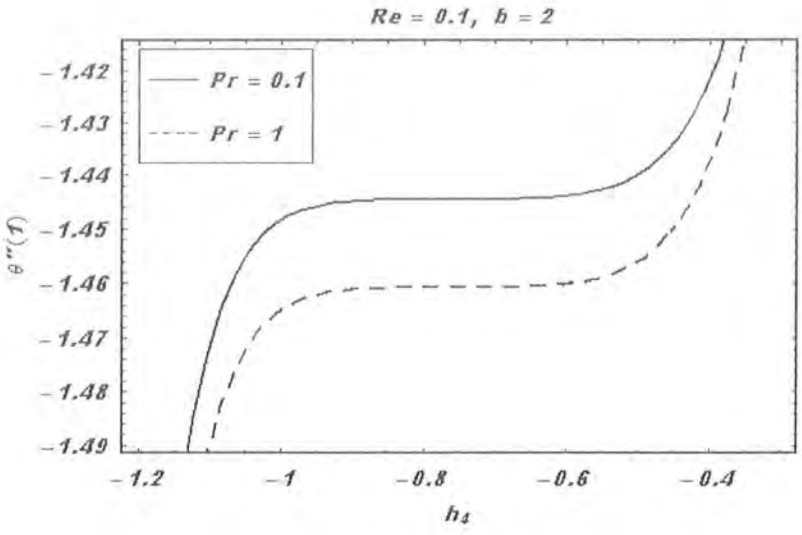

Fig.1.6. h-curves for θ against different Pr.

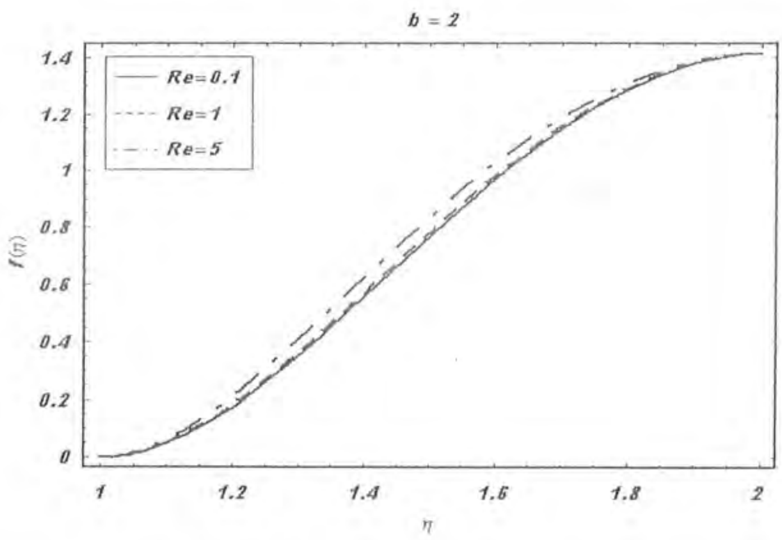

Fig.1.7.Influence of Re over f.

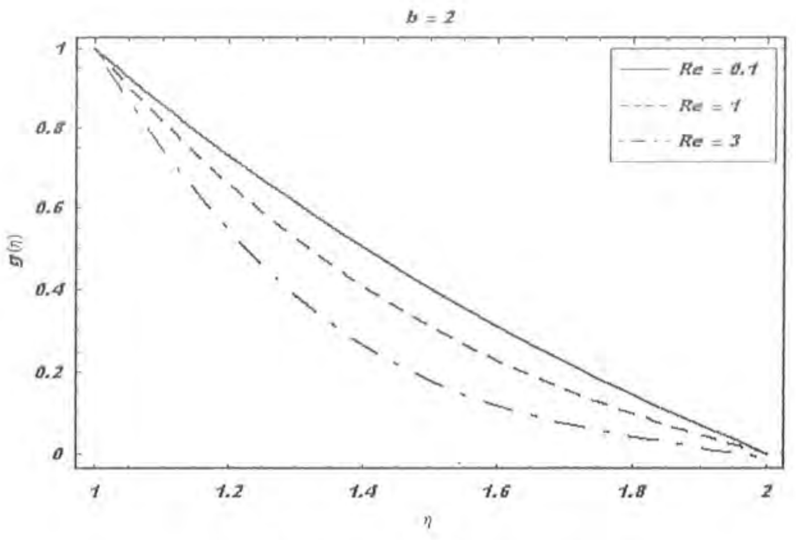

Fig.1.8.Influence of Re over g.

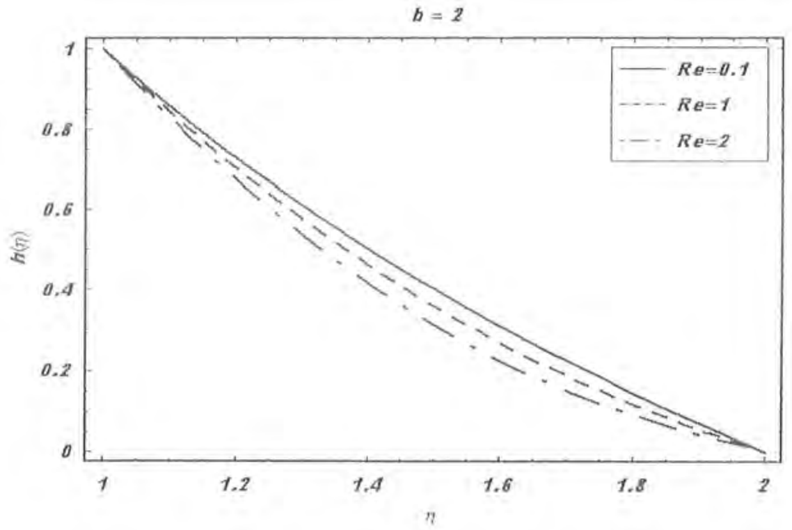

Fig.1.9.Influence of Re over h.

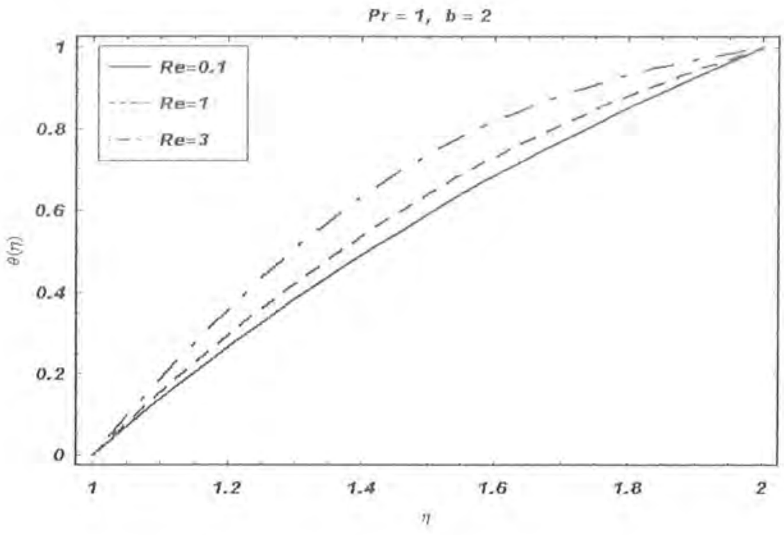

Fig.1.10. Influence of Re over θ.

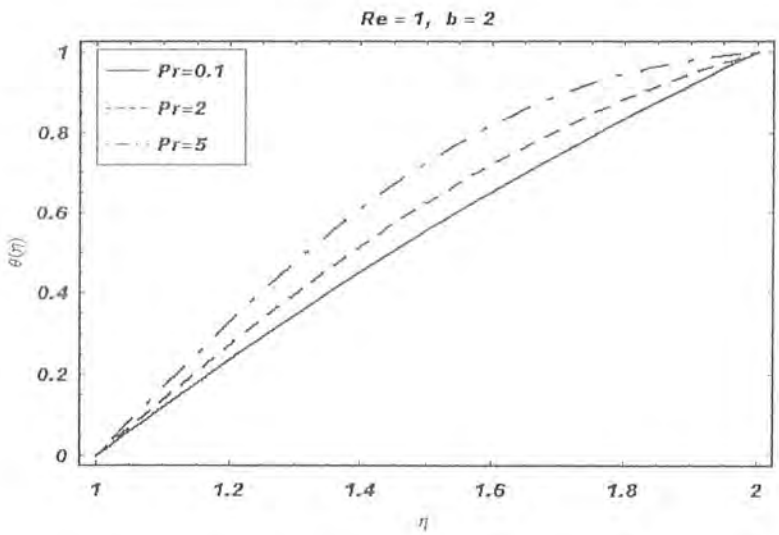

Fig.1.11.Influence of Pr over θ.

1.5 Tables

Re	Numeric	HAM	Small Re	Small gap
0.1	650.3526	650.3526	650.352	650.457
1	654.7679	654.7679	654.770	654.571
10	698.6176	698.6176	698.951	695.714
100	1082.300	1082.3	1140.800	1107.100
1000	2819.700	2819.7		
10000	8447.300	8447.300		

Table 1.1 : Comparison of different solutions for $f''(1)$, $b = 1.1$.

Re	Numeric	HAM	Small Re	Small gap
0.1	11.0010	11.001	11.001	11.0457
1	11.6772	11.6772	11.684	11.4571
10	17.5348	17.5348	18.519	15.5714
100	44.4492	44.4492		
1000	132.436	132.436		
10000	411.373	411.373		

Table 1.2 : Comparison of different solutions for $f''(1)$, $b = 2$.

Re	Numeric	HAM	Small Re	Small gap
0.1	0.667	0.667	0:6674	0.634
1	0.863	0.863	0.8938	0.680
10	1.867	1.867		
100	5.292	5.292		
1000	16.210	16.21		
10000	50.764	50.764		

Table 1.3 : Comparison of different solutions for $f''(1)$, $b = 10$.

Re	Numeric	Ham	Small Re	Small gap
0.1	-13883	-13883	-13883	-13823
1	-14117	-14117	-14116	-14031
10	-16507	-16507	-16452	-16114
100	-42933	-42933	-39806	-36943
1000	-30597	-30597	-273350	-245230
10000	-2813200	-2813200		

Table 1.4 : Comparison of different solutions for $f'''(1)$, $b = 1.1$.

Re	Numeric	Ham	Small Re	Small gap
0.1	-36.1443	-36.1443	-36.143	-30.2314
1	-41.0797	-41.0797	-41.000	-32.3143
10	-93.5670	-93.567	-89.565	
100	-590.738	-590.738	-575.21	
1000	-5211.80	-5211.8	-5431.7	
10000	-50187.0	-50187.0		

Table 1.5 : Comparison of different solutions for $f'''(1)$, $b = 2$.

Re	Numeric	Ham	Small Re	Small gap
0.1	-0.9172	-0.9172	-0.917	-0.241
1	-1.3924	-1.3924	-1.405	-0.267
10	-5.2400	-5.240	-6.287	
100	-36.4750	-36.475		
1000	-322.795	-322.795		
10000	-3102.90	-3102.90		

Table 1.6 : Comparison of different solutions for $f'''(1)$, $b = 10$.

Re	Numeric	Ham	Small Re	Small gap
0.1	-10.5382	-10.5382	-10.538	-10.545
1	-10.9489	-10.9489	-10.948	-10.950
10	-14.6586	-14.6586	-14.658	-15.000
100	-35.7103	-35.7103	-35.710	
1000	-106.9611	-106.9611	-106.961	
10000	-332.1775	-332.1775		

Table 1.7 : Comparison of different solutions for $g'(1)$, $b = 1.1$.

Re	Numeric	Ham	Small Re	Small gap
0.1	-1.4963	-1.4963	-1.496	-1.545
1	-1.9309	-1.9309	-1.984	-1.950
10	-4.3856	-4.3856		-6.000
100	-12.6450	-12.645		
1000	-38.7853	-38.7853		
10000	-121.452	-121.452		

Table 1.8 : Comparison of different solutions for $g'(1)$, $b = 2$.

Re	Numeric	Ham	Small Re	Small gap
0.1	-0.5082	-0.50802	-0.623	-0.626
1	-0.9040	-0.9040	-0.731	-0.761
10	-2.2168	-2.2168	-1.809	
100	-6.3381	-6.3381		
1000	-19.3699	-19.3699		
10000	-60.5821	-60.581		

Table 1.9 : Comparison of different solutions for $g'(1)$, $b = 10$.

Re	Numeric	Ham	Small Re	Small gap
0.1	-10.5151	-10.5151	-10.515	-10.515
1	-10.6511	-10.6511	-10.650	-10.650
10	-12.0407	-12.0407	-12.007	-12.000
100	-24.8226	-24.8226	-25.570	-25.500
1000	-75.1076	-75.1076		
10000	-233.5209	-233.5209		

Table 1.10 : Comparison of different solutions for $h'(1)$, $b = 1.1$.

Re	Numeric	Ham	Small Re	Small gap
0.1	-1.5151	-1.5151	-1.515	-1.515
1	-1.6554	-1.6554	-1.650	-1.650
10	-3.0517	-3.0517	-3.007	-3.000
100	-8.8636	-8.8636		
1000	-27.2421	-27.2421		
10000	-85.3916	-85.3916		

Table 1.11 : Comparison of different solutions for $h'(1)$, $b = 2$.

Re	Numeric	Ham	Small Re	Small gap
0.1	-0.6235	-0.6235	-0.623	-0.626
1	-0.7570	-0.757	-0.731	-0.761
10	-1.5941	-1.5941	-1.809	
100	-4.4487	-4.4487		
1000	-13.5959	-13.5959		
10000	-42.5694	-42.5694		

Table 1.12 : Comparison of different solutions for $h'(1)$, $b = 10$.

Chapter 2

Axisymmetric stagnation flow of a micropolar fluid in a moving cylinder: An analytical solution

2.1 Introduction

In this chapter, we have presented the axisymmetric stagnation flow of a micropolar fluid in a moving cylinder. The governing equations of motions, microrotation and energy are simplified with the help of suitable similarity transformations. System of six nonlinear coupled differential equations have been solved analytically with the help of strong analytical tool known as homotopy analysis method. The physical features of various parameters have been discussed through graphs. Also, a comparison of our analytical solutions and the available numerical results are made in the limiting case. The values of skinfriction and local Nusselt number have been also computed.

2.2 Mathematical formulation

Let us consider an incompressible flow of a micropolar fluid between two cylinders. We are considering cylindrical geometry assuming that the flow is axisymmetric about z-axis. The inner cylinder is of radius R rotating with angular velocity Ω and moving with velocity W in the axial z-direction. The inner cylinder is enclosed by an outer cylinder of radius bR. The fluid is injected radially with velocity U from the outer cylinder towards the inner cylinder. The equations for micropolar fluid in the presence of heat transfer analysis are stated as,

$$\operatorname{div} \mathrm{V} = 0, \tag{2.1}$$

$$\rho \frac{d\mathrm{V}}{dt} = -\nabla p + k\nabla \times \mathrm{w} + (\mu + k)\nabla^2 \mathrm{V}, \tag{2.2}$$

$$\rho j \frac{d\mathrm{w}}{dt} = -2k\mathrm{w} + k\nabla \times \mathrm{V} - \gamma(\nabla \times \nabla \times \mathrm{w}) + (\alpha + \beta + \gamma)\nabla(\nabla \times \mathrm{w}), \tag{2.3}$$

$$\rho c_p \frac{d\sigma}{dt} = \mathrm{T.L} - \operatorname{div} \mathrm{q}, \tag{2.4}$$

where $\mathbf{V}$ is the velocity vector, ρ is the density, $\mathbf{w}$ is the angular microrotation momentum, μ is the dynamic viscosity, k is the vertex viscosity, j is the microrotation density, α, β and γ are the micropolar constants, c_p is the specific heat at constant pressure, σ is the temperature, v is the kinematic viscosity, k^* is the thermal conductivity and p is pressure. We seek the velocity, microrotation and temperature of the following form

$$\mathrm{V}(r,z) = (u(r,z), v(r,z), w(r,z)), \quad \mathrm{w}(r,z) = (0, N^*(r,z), 0), \quad \sigma = \sigma(r,z). \tag{2.5}$$

Making use of $Eq.$ (2.5) into $Eq.$ (2.1) to (2.4) the governing equations in component form become

$$u_r + w_z + \frac{u}{r} = 0, \tag{2.6}$$

$$\rho\left(uu_r + wu_z - \frac{v^2}{r}\right) = -\frac{\partial p}{\partial r} - kN_z^* + (\mu + k)\left(u_{rr} + \frac{1}{r}u_r + u_{zz} - \frac{u}{r^2}\right), \tag{2.7}$$

$$\rho\left(uv_r + wv_z + \frac{uv}{r}\right) = (\mu + k)\left(v_{rr} + \frac{1}{r}v_r + v_{zz} - \frac{v}{r^2}\right), \tag{2.8}$$

$$\rho(uw_r + ww_z) = -\frac{\partial p}{\partial z} + k\left(N_r^* + \frac{N^*}{r}\right) + (\mu + k)\left(w_{rr} + \frac{1}{r}w_r + w_{zz}\right), \tag{2.9}$$

$$\rho j(uN_r^* + wN_z^*) = -2kN^* + k(u_z - w_r) + \gamma\left(N_{rr}^* + \frac{N_r^*}{r} + N_{zz}^* - \frac{N^*}{r^2}\right), \tag{2.10}$$

$$\rho c_p\left(u\sigma_r + w\sigma_z\right) = \mu(2u_r^2 + v_r^2 - \frac{2vv_r}{r} + 2u_z w_r + w_r^2 + \frac{v^2}{r^2} + \frac{2u^2}{r^2}$$
$$+u_z^2 + v_z^2 + 2w_z^2) + k\left(\sigma_{rr} + \frac{1}{r}\sigma_r + \sigma_{zz}\right). \quad (2.11)$$

To eliminate the pressure term from $Eqs.$ (2.7) and (2.9), we apply the cross differentiation method, that gives

$$\rho\left(\left(u_r w_r + u w_{rr} + w_r w_z + w w_{rz}\right) - \left(u u_{rz} + u_r u_z + w u_{zz} + u_z w_z - \frac{2vv_z}{r}\right)\right)$$
$$= k\left(N_{rr}^* + \frac{N_r^*}{r} + N_{zz}^* - \frac{N^*}{r^2}\right) + (\mu + k)\left(w_{rrr} + \frac{1}{r}w_{rr} - \frac{1}{r^2}w_r + w_{rzz} - u_{rrz}\right.$$
$$\left. -\frac{1}{r}u_{rz} - u_{zzz} + \frac{u_z}{r^2}\right). \quad (2.12)$$

The corresponding boundary conditions take the following form

$$\mathrm{V}\left(R, z\right) = \left(0, a\Omega, 0\right), \qquad \mathrm{V}\left(bR, z\right) = \left(-U, 0, 0\right), \quad (2.13)$$

$$N^*\left(R, z\right) = n\tau_{rz}, \qquad N^*\left(bR, z\right) = 0, \quad (2.14)$$

$$\sigma(R, z) = \sigma_1, \quad \sigma(bR, z) = \sigma_2, \quad (2.15)$$

where τ_{rz} is the shear stress and $n = 0$ corresponds to strong concentration of microparticles, $n = \frac{1}{2}$ is the weak concentration of microparticles.

Introducing the following similarity transformations

$$u\left(r, z\right) = \frac{-Uf\left(\eta\right)}{\eta}, \quad v\left(r, z\right) = a\Omega h\left(\eta\right), \quad w\left(r, z\right) = 2Uf'\left(\eta\right)\xi + Wg\left(\eta\right), \quad (2.16)$$

$$N^*\left(r, z\right) = \frac{2U}{R}M\left(\eta\right)\xi + \frac{W}{R}N\left(\eta\right), \quad \theta\left(r, z\right) = \frac{T - T_1}{T_2 - T_1}, \quad (2.17)$$

$$\eta = \frac{r^2}{R^2}, \quad \xi = \frac{z}{R}. \quad (2.18)$$

Making use of $Eqs.$ (2.16) to (2.18) into $Eqs.$ (2.8) and (2.10) to (2.12), we obtain

$$\begin{aligned}
& 4\rho U\left[f''\left(2Uf'\xi+Wg\right)-f\left(2Uf'''\xi+Wg''\right)\right] \\
= & \frac{k}{R\sqrt{\eta}}[4\left(2UM'\xi+WN'\right)+4\eta\left(2UM''\xi+WN''\right)-\frac{1}{\eta}\left(2UM\xi+WN\right)] \\
& +\frac{8\left(\mu+k\right)}{R}\left[\eta\left(2Uf^{iv}\xi+Wg'''\right)+2\left(2Uf'''\xi+Wg''\right)\right], \qquad (2.19)
\end{aligned}$$

$$4\eta h''+4h'-\frac{h}{\eta}+\frac{\mathrm{Re}}{1+K}\left(4fh'+\frac{2fh}{\eta}\right)=0, \qquad (2.20)$$

$$\begin{aligned}
& \frac{2U}{R^2}\rho j\left[f\left(2UM'\xi+WN'\right)+M\left(2Uf'\xi+Wg\right)\right] \\
= & -\frac{2K}{R}\left(2UM\xi+WN\right)-\frac{2K}{R}\sqrt{\eta}\left(2Uf''\xi+Wg'\right) \\
& +\frac{\gamma}{R^3}[4\left(2UM'\xi+WN'\right)+4\eta\left(\left(2UM''\xi+WN''\right)\right) \\
& -\frac{1}{\eta}\left(2UM\xi+WN\right)], \qquad (2.21)
\end{aligned}$$

$$\eta\theta''+\theta'+\mathrm{Pr}\,\mathrm{Re}\,f\theta'=0. \qquad (2.22)$$

Equating the coefficients of like powers of ξ, in $Eqs.$ (2.19) and (2.21), we obtain

$$\begin{aligned}
4\rho U\left(2Uf'f''-2Uff'''\right) &= \frac{k}{R\sqrt{\eta}}\left(8UM'+8U\eta M''-\frac{2}{\eta}UM\right)+ \\
& \frac{8\left(\mu+k\right)}{R}\left(2U\eta f^{iv}+4Uf'''\right), \qquad (2.23)
\end{aligned}$$

$$\begin{aligned}
4\rho U\left(Wf''g-Wfg''\right) &= \frac{k}{R\sqrt{\eta}}\left(4WN'+4\eta WN''-\frac{W}{\eta}N\right)+ \\
& \frac{8\left(\mu+k\right)}{R}\left(\eta Wg'''+2Wg''\right), \qquad (2.24)
\end{aligned}$$

$$\begin{aligned}
\frac{2U}{R^2}\rho j\left[2UfM'+2Uf'M\right] &= -\frac{4KU}{R}M-\frac{4KU}{R}\sqrt{\eta}f'' \\
& +\frac{\gamma}{R^3}(8UM'+8U\eta M''-\frac{2U}{\eta}M), \qquad (2.25)
\end{aligned}$$

$$\frac{2U}{R^2}\rho j\left[WfN' + WMg\right] = -\frac{2K}{R}WN - \frac{2K}{R}\sqrt{\eta}Wg' + \frac{\gamma}{R^3}(4WN' + 4W\eta N'' - \frac{W}{\eta}N). \quad (2.26)$$

Simplification of *Eqs.* (2.23) to (2.26) yield

$$\eta f^{iv} + 2f''' + \frac{\text{Re}}{1+K}\left(ff''' - f'f''\right) + \frac{K}{8(1+K)}\frac{1}{\sqrt{\eta}}\left(4\eta M'' + 4M' - \frac{M}{\eta}\right) = 0, \quad (2.27)$$

$$\eta g'' + g' + \frac{K}{1+K}\left(4\sqrt{\eta}N' + \frac{2}{\sqrt{\eta}}N\right) + \frac{\text{Re}}{1+K}\left(fg' - f'g\right) = 0, \quad (2.28)$$

$$4\eta M'' + 4M' - \frac{M}{\eta} - \frac{4\,\text{Re}}{\Lambda}(fM' + f'M) - \frac{2K\delta}{\Lambda}\left(M + \sqrt{\eta}f''\right) = 0, \quad (2.29)$$

$$4\eta N'' + 4N' - \frac{N}{\eta} - \frac{4\,\text{Re}}{\Lambda}\left(fN' + Mg\right) - \frac{2K\delta}{\Lambda}\left(N + \sqrt{\eta}g'\right) = 0, \quad (2.30)$$

in which $Re = \frac{UR}{2\nu}$ is the cross-flow Reynolds number, $\Lambda = \frac{\gamma}{\mu j}$ is the micropolar coefficient, $\delta = \frac{R^2}{j}$ and $K = \frac{k}{\mu}$ are the micropolar parameters, $\Pr = \frac{\upsilon\rho c_p}{k^*}$ is the Prandle number $Ec = \frac{u^2}{c_p(T_b - T_1)}$ is the Eckert number, $\alpha = \frac{w}{u}$ and $\beta = \frac{a\Omega}{u}$ are the velocity ratios. The boundary conditions in the transformed domain are

$$f(1) = 0, \qquad f'(1) = 0, \qquad f(b) = \sqrt{b}, \qquad f'(b) = 0, \quad (2.31)$$

$$g(1) = 1, \qquad g(b) = 0, \qquad h(1) = 1, \qquad h(b) = 0, \quad (2.32)$$

$$M(1) = -2nf''(1) = -\frac{6\sqrt{b}n}{(b-1)^3}(b-\eta), \qquad M(b) = 0, \quad (2.33)$$

$$N(1) = -2nf''(1) = -\frac{6\sqrt{b}n}{(b-1)^3}(b-\eta), \qquad N(b) = 0, \quad (2.34)$$

$$\theta(1) = 0, \qquad \theta(b) = 1. \quad (2.35)$$

Eqs. (2.20), (2.22) and (2.27) to (2.30) are highly nonlinear coupled equations and are solved analytically with the help of homotopy analysis method.

2.3 Solution of the problem by Homotopy analysis method

The solution of the above boundary value problem is obtained with the help of HAM. For HAM solution, we choose the initial guesses as [26-36]

$$f_0(\eta) = \frac{\sqrt{b}}{b-1}((3b-1) - 6b\eta + 3(b+1)\eta^2 - 2\eta^3, \tag{2.36}$$

$$g_0(\eta) = \frac{b-\eta}{b-1}, \qquad h_0(\eta) = \frac{b-\eta}{b-1}, \tag{2.37}$$

$$M_0(\eta) = \frac{-6\sqrt{b}n}{(b-1)^3}(b-\eta), \qquad N_0(\eta) = \frac{2n}{(b-1)^2}(b-\eta), \tag{2.38}$$

$$\theta_0(\eta) = \frac{\eta-1}{b-1}. \tag{2.39}$$

The corresponding auxiliary linear operators are

$$L_f = \frac{d^4}{d\eta^4}, \quad L_g = \frac{d^2}{d\eta^2}, \quad L_h = \frac{d^2}{d\eta^2}, \tag{2.40}$$

$$L_M = \frac{d^2}{d\eta^2}, \quad L_N = \frac{d^2}{d\eta^2}, \quad L_\theta = \frac{d^2}{d\eta^2}, \tag{2.41}$$

which satisfy

$$L_f[c_1 + c_2\eta + c_3\eta^2 + c_4\eta^3] = 0, \tag{2.42}$$

$$L_g[c_5 + c_6\eta] = 0, \quad L_h[c_7 + c_8\eta] = 0, \tag{2.43}$$

$$L_M[c_9 + c_{10}\eta] = 0, \quad L_N[c_{11} + c_{12}\eta] = 0, \tag{2.44}$$

$$L_\theta[c_{13} + c_{14}\eta] = 0, \tag{2.45}$$

where c_i $(i = 1, ..., 14)$ are arbitrary constants while the zeroth-order deformation equations are defined as

$$(1-p)\, L_f[\hat{f}(\eta;p) - f_0(\eta)] = p\hbar_1 N_f[\hat{f}(\eta;p)], \tag{2.46}$$

$$(1-p)\, L_g[\hat{g}(\eta;p) - g_0(\eta)] = p\hbar_2 N_g[\hat{g}(\eta;p)], \tag{2.47}$$

$$(1-p)\, L_h[\hat{h}(\eta;p) - h_0(\eta)] = p\hbar_3 N_h[\hat{h}(\eta;p)], \tag{2.48}$$

$$(1-p)\,L_M[\hat{M}(\eta;p)-M_0(\eta)]=p\hbar_4 N_M[\hat{M}(\eta;p)], \tag{2.49}$$

$$(1-p)\,L_N[\hat{N}(\eta;p)-N_0(\eta)]=p\hbar_5 N_N[\hat{N}(\eta;p)], \tag{2.50}$$

$$(1-p)\,L_\theta[\hat{\theta}(\eta;p)-\theta_0(\eta)]=p\hbar_6 N_\theta[\hat{\theta}(\eta;p)], \tag{2.51}$$

where

$$N_f[\hat{f}(\eta;p)]=\eta\hat{f}^{iv}+2\hat{f}'''+\frac{\mathrm{Re}}{(1+K)}(\hat{f}\hat{f}'''-\hat{f}'\hat{f}'')+\frac{K}{8(1+K)\sqrt{\eta}}\left(4\eta\hat{M}''+4\hat{M}'-\frac{\hat{M}}{\eta}\right), \tag{2.52}$$

$$N_g[\hat{g}(\eta;p)]=\eta g''+g'+\frac{\mathrm{Re}}{(1+K)}\left(\hat{f}\hat{g}'-\hat{f}'\hat{g}\right)+\frac{K}{(1+K)}\sqrt{\eta}\left(4\hat{N}'+\frac{2\hat{N}}{\eta}\right), \tag{2.53}$$

$$N_h[\hat{h}(\eta;p)]=4\eta\hat{h}''+4\hat{h}'-\frac{\hat{h}}{\eta}+\frac{\mathrm{Re}}{(1+K)}\left(4\hat{f}\hat{h}'+\frac{2\hat{f}\hat{h}}{\eta}\right), \tag{2.54}$$

$$N_M[\hat{M}(\eta;p)]=4\eta\hat{M}''+4\hat{M}'-\frac{\hat{M}}{\eta}-\frac{4\,\mathrm{Re}}{\Lambda}(\hat{f}\hat{M}'+\hat{f}'\hat{M})-\frac{2K\delta}{\Lambda}\left(\hat{M}+\sqrt{\eta}\hat{f}''\right), \tag{2.55}$$

$$N_N[\hat{N}(\eta;p)]=4\eta\hat{N}''+4\hat{N}'-\frac{\hat{N}}{\eta}-\frac{4\,\mathrm{Re}}{\Lambda}\left(\hat{f}\hat{N}'+\hat{M}\hat{g}\right)-\frac{2K\delta}{\Lambda}\left(\hat{N}+\sqrt{\eta}\hat{g}'\right), \tag{2.56}$$

$$N_\theta[\hat{\theta}(\eta;p)]=\eta\hat{\theta}''+\hat{\theta}'+\mathrm{Pr}\,\mathrm{Re}\,\hat{f}\hat{\theta}'. \tag{2.57}$$

The boundary conditions for the zeroth order system are defined as

$$\hat{f}(1;p)=0,\ \hat{f}'(1;p)=0,\ \hat{g}(1;p)=1,\ \hat{h}(1;p)=1,\ \hat{\theta}(1;p)=0, \tag{2.58}$$

$$\hat{f}(b;p)=\sqrt{b},\ \hat{f}'(b;p)=0,\ \hat{g}(b;p)=0,\ \hat{h}(b;p)=0,\ \hat{\theta}(b;p)=1, \tag{2.59}$$

$$\hat{M}(1;p)=-2nf_0''(1),\quad \hat{M}(b;p)=0,\quad \hat{N}(1;p)=2ng_0'(1),\quad \hat{N}(b;p)=0. \tag{2.60}$$

The mth order deformation equations can be obtained by differentiating the zeroth-order deformation equations $(2.46-2.51)$ and the boundary conditions $(2.58-2.60)$, m-times with respect to p, then dividing by $m!$, and finally setting $p=0$, we get

$$L_f[f_m(\eta)-\chi_m f_{m-1}(\eta)]=\hbar_1 R_{mf}(\eta), \tag{2.61}$$

$$L_g[g_m(\eta) - \chi_m g_{m-1}(\eta)] = \hbar_2 R_{mg}(\eta), \tag{2.62}$$

$$L_h[h_m(\eta) - \chi_m h_{m-1}(\eta)] = \hbar_3 R_{mh}(\eta), \tag{2.63}$$

$$L_M[M_m(\eta) - \chi_m M_{m-1}(\eta)] = \hbar_4 R_{mM}(\eta), \tag{2.64}$$

$$L_N[N_m(\eta) - \chi_m N_{m-1}(\eta)] = \hbar_5 R_{mN}(\eta), \tag{2.65}$$

$$L_\theta[\theta_m(\eta) - \chi_m \theta_{m-1}(\eta)] = \hbar_6 R_{m\theta}(\eta), \tag{2.66}$$

$$f_m(1) = 0, \quad f_m'(1) = 0, \quad g_m(1) = 0, \quad h_m(1) = 0, \quad \theta_m(1) = 0, \tag{2.67}$$

$$f_m(b) = 0, \quad f_m'(b) = 0, \quad g_m(b) = 0, \quad h_m(b) = 0, \quad \theta_m(b) = 0, \tag{2.68}$$

$$M_m(1) = 0, \quad M_m(b) = 0, \quad N_m(1) = 0, \quad N_m(b) = 0, \tag{2.69}$$

where

$$R_{mf}(\eta) = \eta f_{m-1}'''' + 2f_{m-1}''' + \frac{\mathrm{Re}}{1+K}\sum_{i=0}^{m}(f_i f_{m-1-i}''' - f_i' f_{m-1-i}'') \tag{2.70}$$

$$+\frac{K}{8(1+K)\sqrt{\eta}}\left(4\eta M_{m-1}'' + 4M_{m-1}' - \frac{M_{m-1}}{\eta}\right), \tag{2.1}$$

$$R_{mg}(\eta) = \eta g_{m-1}'' + g_{m-1}' + \frac{\mathrm{Re}}{1+K}\sum_{i=0}^{m}(f_i g_{m-1-i}' - f_i' g_{m-1-i}) \tag{2.71}$$

$$+\frac{K}{1+K}\sqrt{\eta}\left(4N_{m-1}' + \frac{2}{\eta}N_{m-1}\right), \tag{2.2}$$

$$R_{mh}(\eta) = 4\eta h_{m-1}'' + 4h_{m-1}' - \frac{h_{m-1}}{\eta} + \frac{\mathrm{Re}}{1+K}\sum_{i=0}^{m}(4\eta f_i h_{m-1-i}' + \frac{2f_i h_{m-1-i}}{\eta}), \tag{2.72}$$

$$R_{mM}(\eta) = 4\eta M_{m-1}'' + 4M_{m-1}' - \frac{M_{m-1}}{\eta} - \frac{4\,\mathrm{Re}}{\Lambda}\sum_{i=0}^{m}(f_i M_{m-1-i}' + f_i' M_{m-1-i}) \tag{2.73}$$

$$-\frac{2K\delta}{\Lambda}\left(M_{m-1} + \sqrt{\eta} f_{m-1}''\right), \tag{2.3}$$

$$R_{mN}(\eta) = 4\eta N''_{m-1} + 4N'_{m-1} - \frac{N_{m-1}}{\eta} - \frac{4\,\mathrm{Re}}{\Lambda}\sum_{i=0}^{m}\left(f_i N'_{m-1-i} + M_i g_{m-1-i}\right) \tag{2.74}$$

$$-\frac{2K\delta}{\Lambda}\left(N_{m-1} + \sqrt{\eta}g'_{m-1}\right), \tag{2.4}$$

$$R_{m\theta}(\eta) = \eta\theta''_{m-1} + \theta'_{m-1} + \Pr\mathrm{Re}\sum_{i=0}^{m} f_i\theta'_{m-1-i}, \tag{2.75}$$

$$\chi_m = \begin{cases} 0 & m \leq 1 \\ 1 & m > 1. \end{cases} \tag{2.76}$$

With the help of software MATHEMATICA, the solutions of *Eqs.* (2.20) , (2.22) and (2.27) to (2.30) subject to the boundary conditions (2.31) to (2.35) can be defined as

$$f(\eta) = \lim_{Q\to\infty}\left[\sum_{m=1}^{Q} f_m(\eta)\right], \quad g(\eta) = \lim_{Q\to\infty}\left[\sum_{m=1}^{Q} g_m(\eta)\right], \tag{2.77}$$

$$h(\eta) = \lim_{Q\to\infty}\left[\sum_{m=1}^{Q} h_m(\eta)\right], \quad \theta(\eta) = \lim_{Q\to\infty}\left[\sum_{m=1}^{Q} \theta_m(\eta)\right], \tag{2.78}$$

$$M(\eta) = \lim_{Q\to\infty}\left[\sum_{m=1}^{Q} M_m(\eta)\right], \quad N(\eta) = \lim_{Q\to\infty}\left[\sum_{m=1}^{Q} N_m(\eta)\right], \tag{2.79}$$

where

$$f_m(\eta) = f_m^*(\eta) + C_1 + C_2\eta + C_3\eta^2 + C_4\eta^3, \tag{2.80}$$

$$g_m(\eta) = g_m^*(\eta) + C_5 + C_6\eta, \quad h_m(\eta) = h_m^*(\eta) + C_7 + C_8\eta, \tag{2.81}$$

$$M_m(\eta) = M_m^*(\eta) + C_9 + C_{10}\eta, \quad N_m(\eta) = N_m^{**}(\eta) + C_{11} + C_{12}\eta \tag{2.82}$$

$$\theta_m(\eta) = \theta_m^*(\eta) + C_{13} + C_{14}\eta. \tag{2.83}$$

In which $f_m^*(\eta), g_m^*(\eta), h_m^*(\eta), M_m^*(\eta), N_m^{**}(\eta)$ and $\theta_m^*(\eta)$, are the special solutions and can be stated as

$$f_m(\eta) = \sum_{n=1}^{\infty} a_{mn}\eta^{\frac{11}{2}n+3}, \qquad g_m(\eta) = \sum_{n=1}^{\infty} b_{mn}\eta^{\frac{11}{2}n}, \tag{2.84}$$

$$h_m(\eta) = \sum_{n=1}^{\infty} c_{mn}\eta^{\frac{1}{2}(11n+1)}, \qquad M_m(\eta) = \sum_{n=1}^{\infty} d_{mn}\eta^{\frac{11}{2}n-1}, \tag{2.85}$$

$$N_m^*(\eta) = \sum_{n=1}^{\infty} e_{mn}\eta^{\frac{1}{2}(11n-5)}, \qquad \theta_m(\eta) = \sum_{n=1}^{\infty} i_{mn}\eta^{\frac{1}{2}(11n-1)}, \tag{2.86}$$

where a_{mn}, b_{mn}, c_{mn}, d_{mn}, e_{mn}, i_{mn}, are all constants and the numerical date of these above solutions have been computed with the help of Mathematica and shown through graphs.

2.4 Results and discussion

In this section we have discussed the HAM solutions graphically. Therefore, we have plotted the velocities, microrotation and temperature fields for different physical parameters. To discuss the convergence of the series solutions we have plotted the h-curves $(see\ figs.1\ to\ 5)$ It is seen that the convergence region of f is much smaller then the other functions. The nondimensional velocity f for various values of $\mathrm{Re}, \delta, K,$ and Λ are shown in $Figs.$6 to 9. It is observed that with the increase in all the parameters, f increases in the given domain. Moreover, the behavior in all the cases are almost similar. The nondimensional velocities g and h for different values of Re are shown in $Figs.$10 and 11. It is depicted that in the given domain both functions decreases with the increase in Re. Almost similar behavior appeared for δ and K which are not shown here. The effects $\mathrm{Re}, \delta, K,$ and Λ on nondimensional microrotation components M and N are represented in $Figs.$12 to 19. It is observed that both the functions M and N increases with the increase in Re, δ and K, however, with the increase in Λ, M increases but N gives opposite result. It means that with the increase in Λ, N decreases and the maximum value occurs in the middle of the domain.

A comparison of our HAM solutions and available numerical solutions [14] without microrotation effects are shown in tables 2.1 to 2.4. It is seen that both the solutions are almost identical. The HAM solutions for different values of Re/K and Re/α for the weak concentration case $\left(n = \frac{1}{2}\right)$ are given in tables 2.5 to 2.8. The value of skinfriction coefficient is computed in tables 2.9 and 2.10. It is seen that with the increase in Re, the skinfriction coefficient decreases, however the magnitude of skinfriction increases with the increase in α. The effect of Pr and Re on Nusselt numbers are given in table 2.11. It is concluded that with the increase in both Pr and Re, increases the Nusselt number.

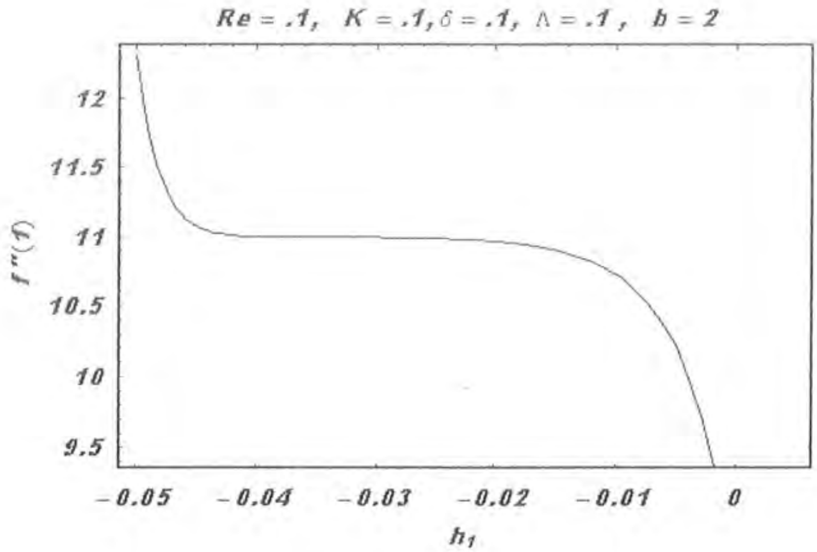

$Fig.2.1.$ h curve of f .

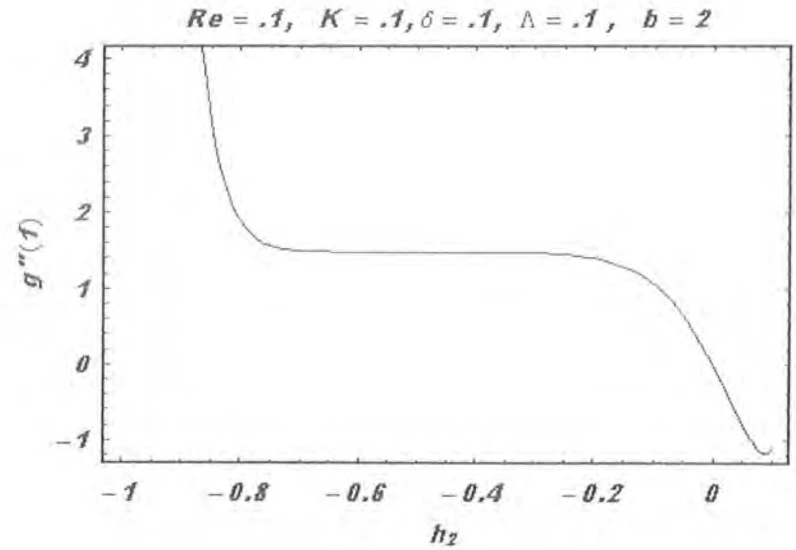

$Fig.2.2.$ h curve of g .

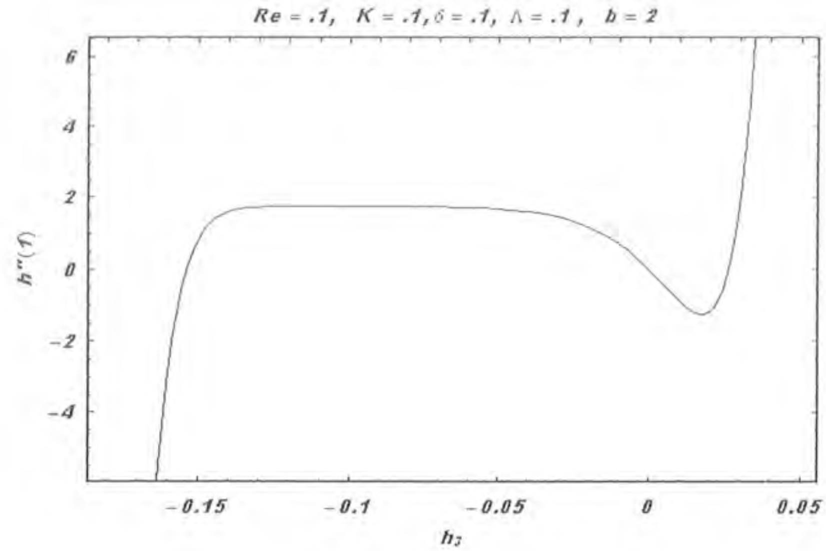

$Fig.2.3.$ h curve of h .

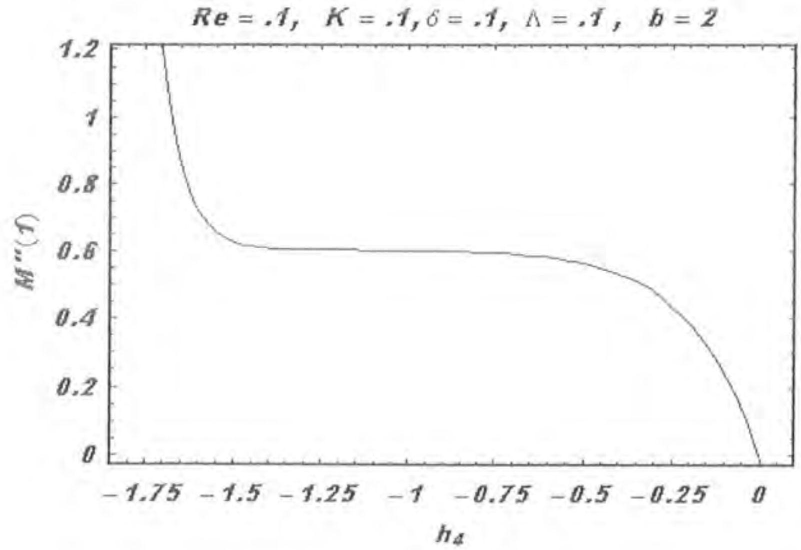

$Fig.2.4.$ h curve of M .

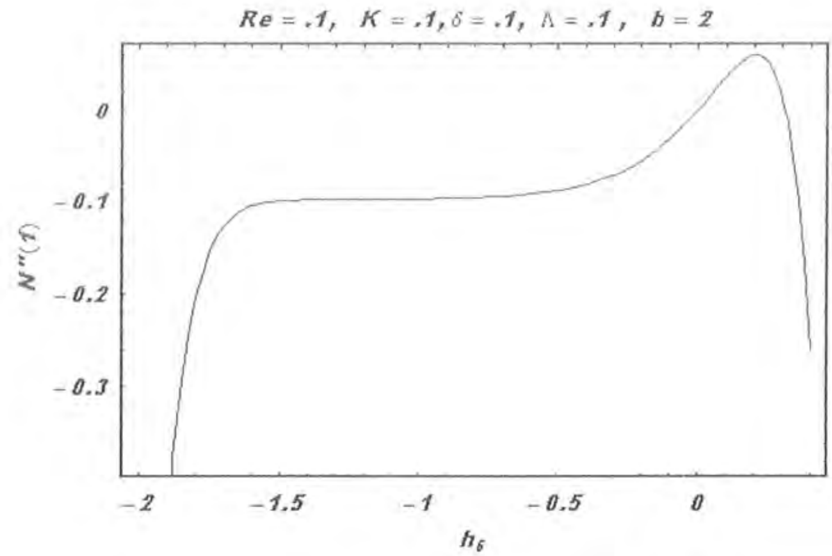

Fig.2.5. h curve of N .

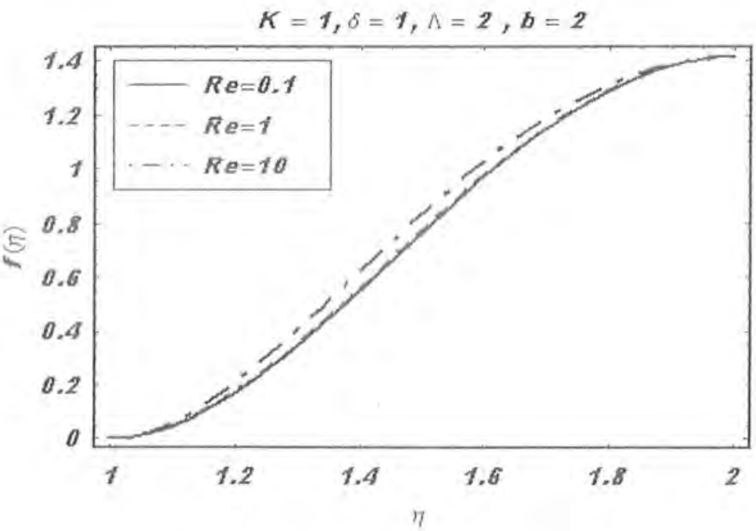

Fig.2.6. Influence of Re over f .

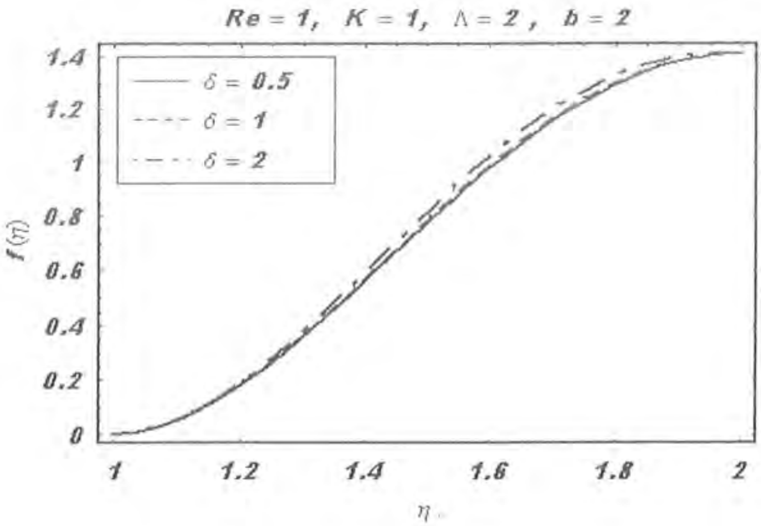

Fig.2.7. Influence of δ over f .

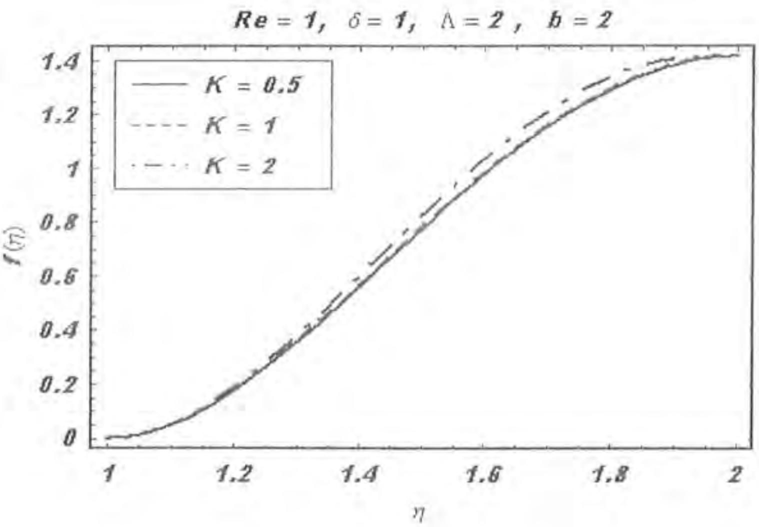

Fig.2.8. Influence of K over f .

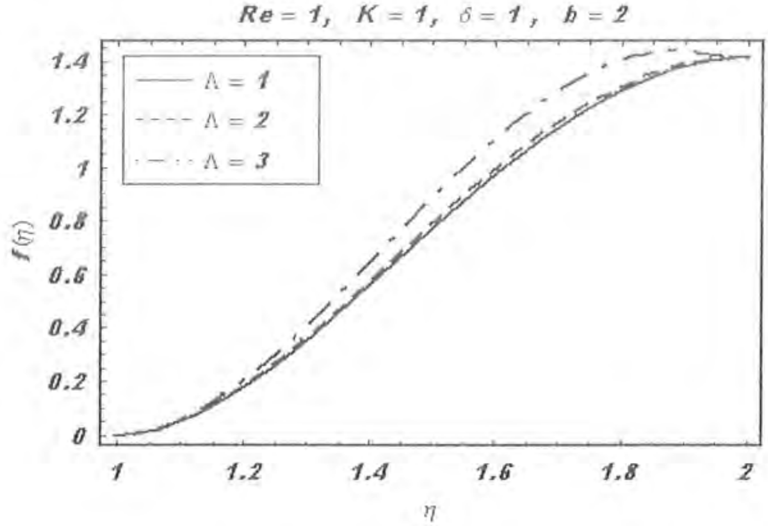

Fig.2.9. Influence of Λ over f .

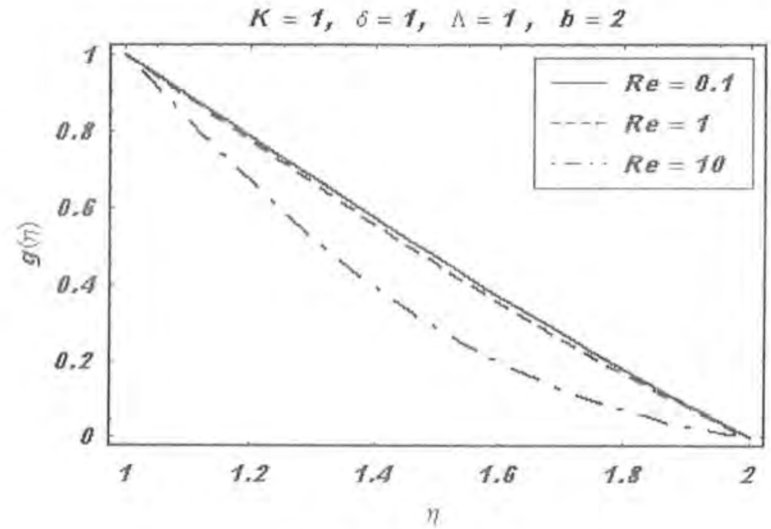

Fig.2.10. Influence of Re over g.

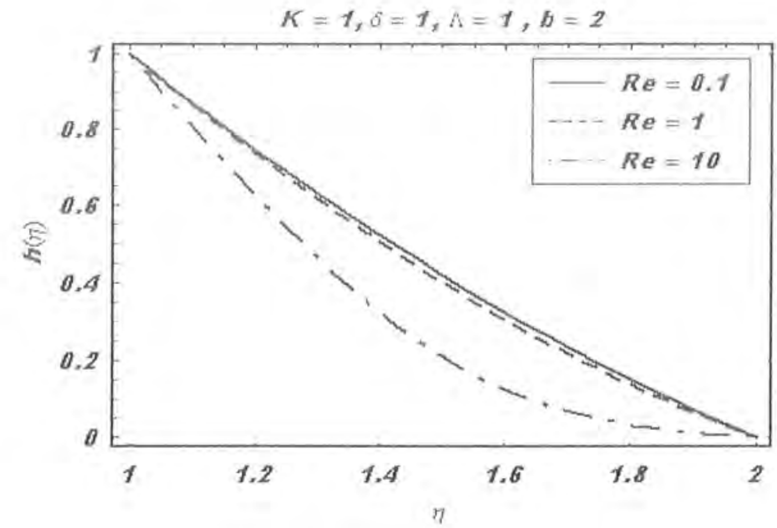

Fig.2.11. Influence of Re over h .

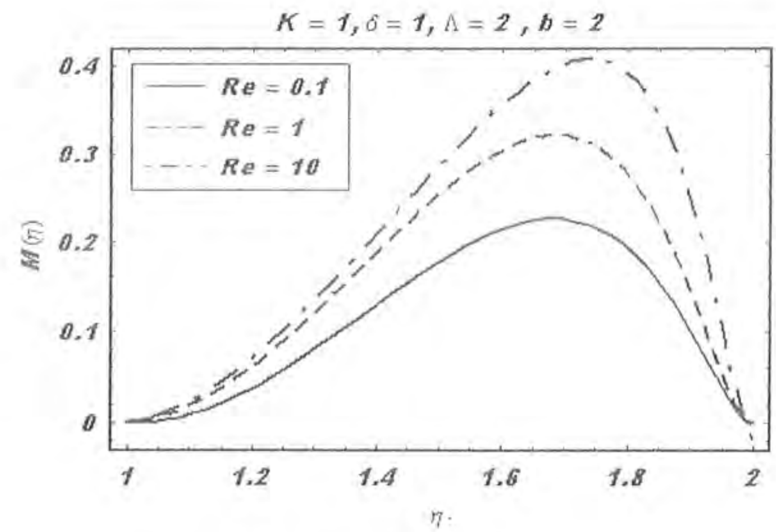

Fig.2.12. Influence of Re over M .

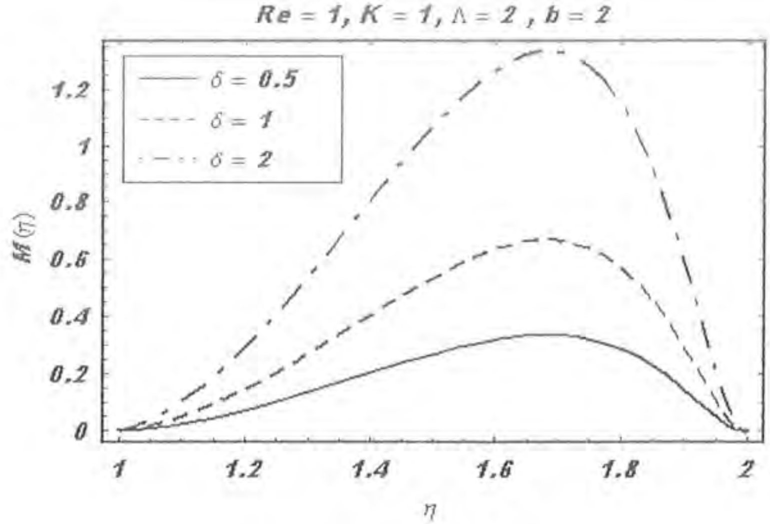

Fig.2.13. Influence of δ over M .

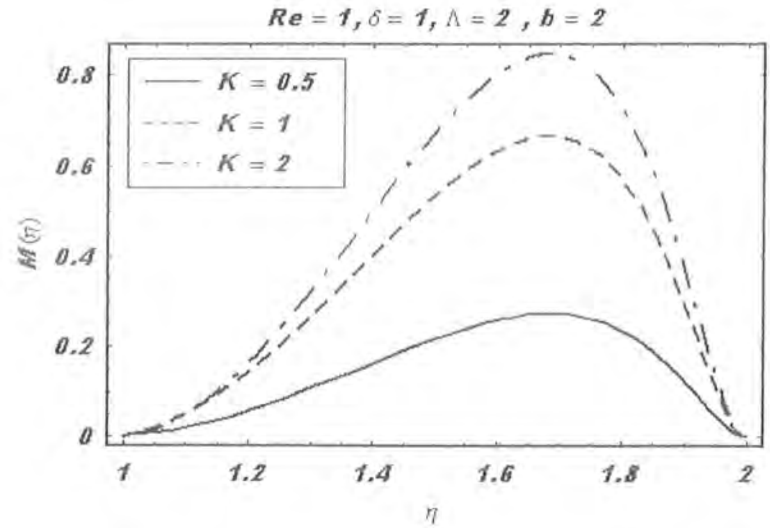

Fig.2.14. Influence of K over M .

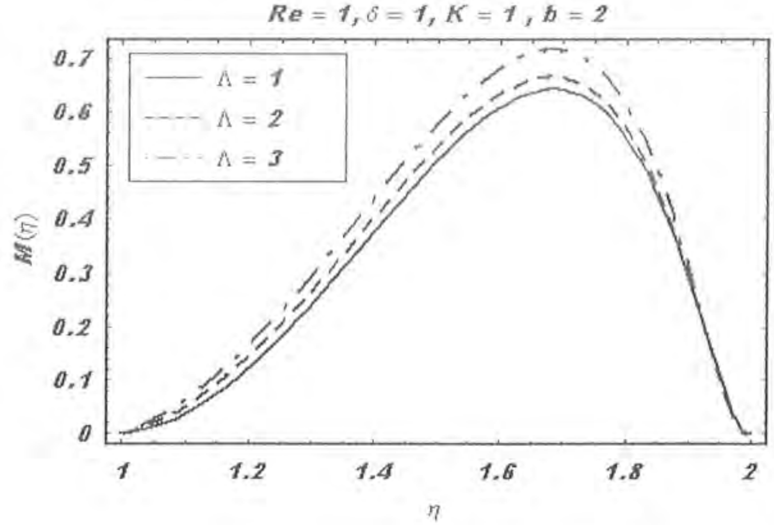

Fig.2.15. Influence of Λ over M .

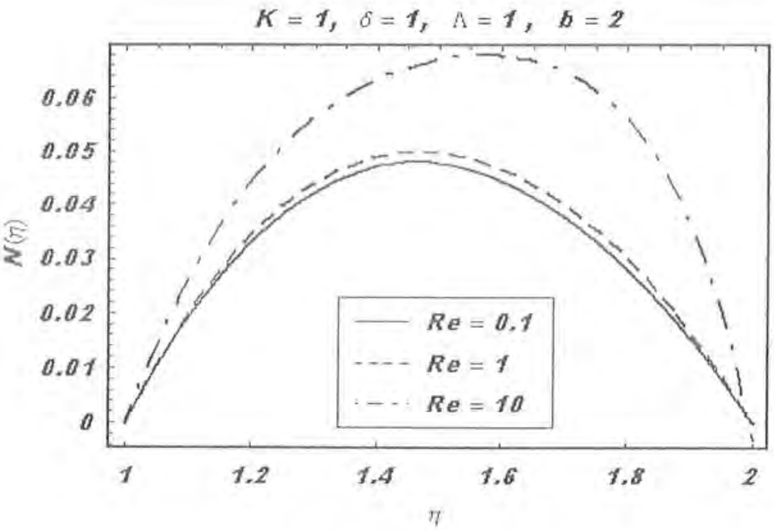

Fig.2.16. Influence of Re over N .

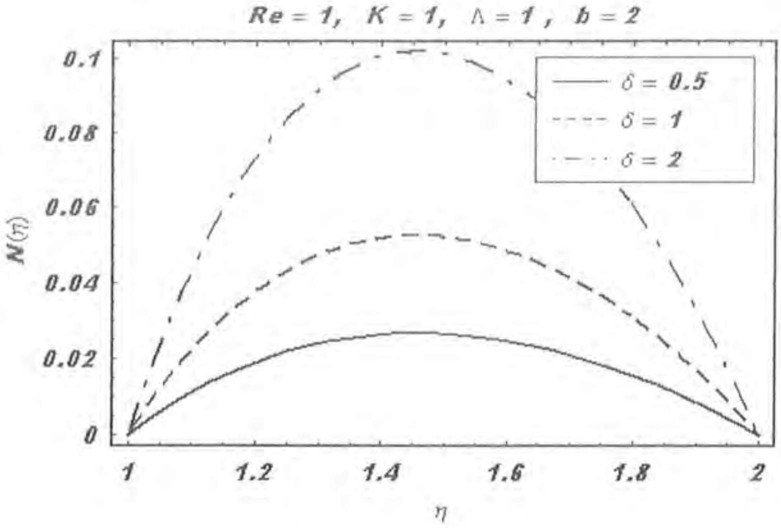

$Fig.$2.17. Influence of δ over N .

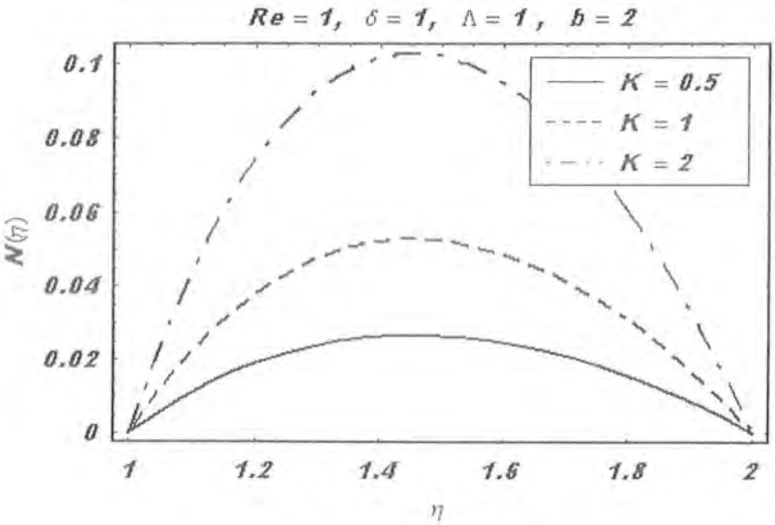

$Fig.$2.18. Influence of K over N .

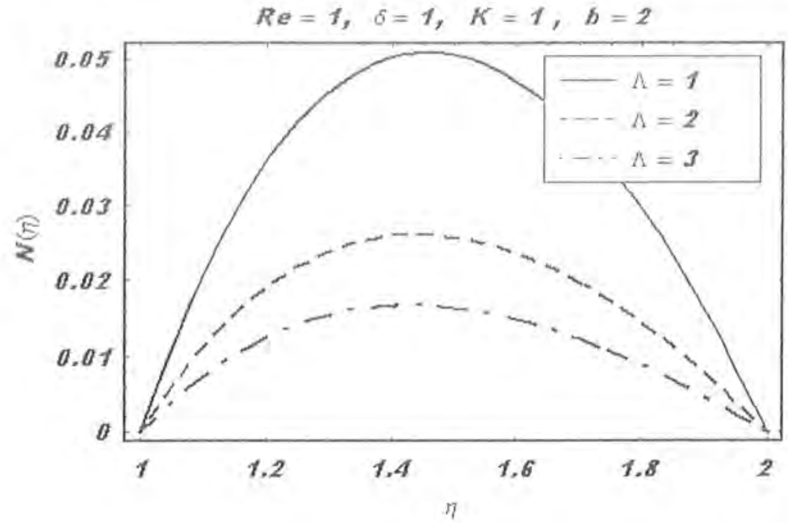

Fig.2.19. Influence of Λ over N .

2.5 Tables

$f''(1)$	b=1.1		b=2		b=10	
Re	Numeric	HAM	Numeric	HAM	Numeric	HAM
0.1	650.3526	650.3526	11.0010	11.001	0.667	0.667
1	654.7679	654.7679	11.6772	11.6772	0.863	0.863
10	698.6176	698.6176	17.5348	17.5348	1.867	1.867
100	1082.300	1082.3	44.4492	44.4492	5.292	5.292
1000	2819.700	2819.7	132.436	132.436	16.210	16.21
10000	8447.300	8447.300	411.373	411.373	50.764	50.764

Table 2.1 : Comparison of numerical and HAM solutions for f''

$f'''(1)$	$b = 1.1$		$b = 2$		b=10	
	Numeric	Ham	Numeric	Ham	Numeric	Ham
0.1	-13883	-13883	-36.1443	-36.1443	-0.9172	-0.9172
1	-14117	-14117	-41.0797	-41.0797	-1.3924	-1.3924
10	-16507	-16507	-93.5670	-93.567	-5.2400	-5.240
100	-42933	-42933	-590.738	-590.738	-36.4750	-36.475
1000	-30597	-30597	-5211.80	-5211.8	-322.795	-322.795
10000	-2813200	-2813200	-50187.0	-50187.0	-3102.90	-3102.90

Table 2.2 : Comparison of numerical and HAM solutions for f'''

$g'(1)$	b=1.1		b=2		b=10	
	Numeric	Ham	Numeric	Ham	Numeric	Ham
0.1	-10.5382	-10.5382	-1.4963	-1.4963	-0.5082	-0.50802
1	-10.9489	-10.9489	-1.9309	-1.9309	-0.9040	-0.9040
10	-14.6586	-14.6586	-4.3856	-4.3856	-2.2168	-2.2168
100	-35.7103	-35.7103	-12.6450	-12.645	-6.3381	-6.3381
1000	-106.9611	-106.9611	-38.7853	-38.7853	-19.3699	-19.3699
10000	-332.1775	-332.1775	-121.452	-121.452	-60.5821	-60.581

Table 2.3 : Comparison of numerical and HAM solutions for g'

$h'(1)$	b=1.1		b=2		b=10	
	Numeric	Ham	Numeric	Ham	Numeric	Ham
0.1	-10.5151	-10.5151	-1.5151	-1.5151	-0.6235	-0.6235
1	-10.6511	-10.6511	-1.6554	-1.6554	-0.7570	-0.757
10	-12.0407	-12.0407	-3.0517	-3.0517	-1.5941	-1.5941
100	-24.8226	-24.8226	-8.8636	-8.8636	-4.4487	-4.4487
1000	-75.1076	-75.1076	-27.2421	-27.2421	-13.5959	-13.5959
10000	-233.5209	-233.5209	-85.3916	-85.3916	-42.5694	-42.5694

Table 2.4 : Comparison of numerical and HAM solutions for h'

	$f''(1)$			$f'''(1)$		
Re \ K	0.1	1	10	0.1	1	10
0.1	10.6248	10.9226	10.9767	-35.1614	-35.6057	-34.9954
1	10.8884	11.2736	11.0673	-38.9314	-38.391	-35.6904
10	14.4853	14.8359	11.9967	-53.9706	-66.9097	-42.7841
100	49.7517	52.1987	20.4853	-592.757	-613.446	-79.9706

Table 2.5 : HAM solutions for f'' and f''' with $n = \frac{1}{2}$

	$g'(1)$			$h'(1)$		
Re \ K	0.1	1	10	0.1	1	10
0.1	-0.745496	-6.99531	-28.7456	-1.91888	-1.98559	-1.73216
1	-0.914615	-90.5488	-298.913	-6.24664	-8.51224	-4.40584
10	-3.3125	-1326.24	-2166.44	-31.5987	-45.5316	-27.1184
100	-16.001	-16384	-587776	98304	14828.9	948.473

Table 2.6 : HAM solutions for g' and h' with $n = \frac{1}{2}$

	$M'(1)$			$N'(1)$		
$\mathrm{Re}\backslash K$	0.1	1	10	0.1	1	10
0.1	-36.5908	-41.1913	-48.3764	-36.3715	118.023	331.351
1	-39.083	-46.4411	-60.245	-48.2935	1725.26	3554.21
10	-48.6085	-51.5855	-47.1489	237.278	14440.5	63401.5
100	-384437	-460888	-538325	-933888	131072	803520

Table 2.7 : HAM solutions for M' and N' with $n = \frac{1}{2}$

$\mathrm{Re}\backslash\alpha$	0	1	2
0.1	353.767	412.605	389.131
1	35.7919	43.1997	39.2168
5	7.52431	10.052	9.37826
10	3.98706	8.35246	5.52623
25	1.85416	3.17628	2.95707

Table 2.8 : Variation of skin friction coefficient for different values of Re/α. $n = 0,\ K = 0, \xi = 1,$

$\mathrm{Re}\backslash\alpha$	0	1	2
0.1	432.517	-806.22	-2027.39
1	44.6699	-1754.12	-3550.89
5	10.1557	-5764.42	-11538.4
10	5.77893	-13304.9	-26615.1
25	2.95237	-33918.7	-79504.9

Table 2.9 : Variation of skin friction coefficient for different values of Re/α. $n = \frac{1}{2},\ K = 1, \xi = 1,$

Re \ α	0	1	2
0.1	438.586	-2241.65	-2257.97
1	44.7221	-3167.3	-3154.96
5	9.70786	-6364.88	-6328.78
10	5.30747	-11903.3	-11820.3
25	2.56233	-36620.5	-36235.1

Table 2.10 : Variation of skin friction coefficient for different values of Re/α. $n = \frac{1}{2}$, $K = 3, \xi = 1$,

Pr\ Re	0.1	1	10	100	1000	10000
0.7	6.27005	6.28002	6.36	6.47	6.53	6.55
7	10.0801	10.180	10.86	12.06	12.75	13.01
70	22.360	22.72	25.25	31.1601	36.38	39.05
700	48.52	49.40	55.86	73.07	95.10	112.80

Table 2.11 : HAM results of Nusselt numbers for different values of Pr/Re, for $K = 0$.

Bibliography

[1] F. Labropulu, D. Lia, Stagnation-point flow of a second-grade fluid with slip, Int J Non-Linear Mec, 43 (2008) 941-947.

[2] V. Kumarana, R. Tamizharasia, K. Vajravelub, Approximate analytic solutions of stagnation point flow in a porous medium, Comm Nonlinear Sci Num Simu, 14 (2009) 2677-2688.

[3] C. Y. Wang, axisymmetric stagnation flow on a cylinder, Quart. Appl. Math, 32 (1974) 207-213.

[4] C. Y. Wang, Off-centered stagnation flow towards a rotating disc, Int. J. Engag. Sci. 46 (2008) 391-396.

[5] C. Y. Wang, Stagnation slip flow and heat transfer on a moving plate, Che. Eng. Sci, 61 (2006) 7668-7672.

[6] C. Y. Wang, Axisymmetric stagnation flow towards a moving plate, A. I. Ch. E. Journal 19 (1973) 1080–1080.

[7] C. Y. Wang, Similarity stagnation point solutions of the Navier–Stokes equations – review and extension, Euro J Mech B/Fluids, 27 (2008) 678-683.

[8] C. Y. Wang, Stagnation flow towards a shrinking sheet, Int J Non-Linear Mech, 43 (2008) 377-382.

[9] R. Nazara, N. Amina, D. Filipb and I. Pop, Stagnation point flow of a micropolar fluid towards a stretching sheet. Int J Non-Linear Mech, 39 (2004) 1227-1235.

[10] Y. Y. Loka, N. Amin, I. Pop, Unsteady boundary layer flow of a micropolar fluid near the rear stagnation point of a plane surface, Int J Thermal Sci, 42 (2003) 995-1001.

[11] F. Labropulu, D. Li, I. Pop, Non-orthogonal stagnation-point flow towards a stretching surface in a non-Newtonian fluid with heat transfer, Int. J. Ther. Sci,

[12] K. Hiemenz, Die Grenzschicht an einem in den gleichformingen Flussigkeitsstrom eingetauchten graden Kreiszylinder, Dinglers Polytech. J. 326 (1911) 321-324.

[13] F. Homann, Der Einfluss grosser Z¨ahighkeit bei der Str¨omung um den Zylinder und um die Kugel. Zeitschrift fur angewandte Mathematik und Mechanik 16 (1936) 153-164.

[14] L. Hong, C.Y. Wang, Annular axisymmetric stagnation flow on a moving cylinder, Int. J. Engag. Sci. 47 (2009) 141-152.

[15] S. Heller, W. Shapiro, O. Decker, A porous hydrostatic gas bearing for use in miniature turbomachinery, ASLE Trans. 22 (1971) 144-155.

[16] B. C. Majumdar, Analysis of externally pressurized porous gas bearings-1, Wear 33 (1975) 25-35.

[17] A. C. Eringen, Theory of micropolar fluids, J. Math. Mech. 16 (1966) 1-18.

[18] A. C. Eringen, J. Math. Anal. Appl. 38 (1972) 480.

[19] Chun-I Chen, Non-linear stability characterization of the thin micropolar liquid film flowing down the inner surface of a rotating vertical cylinder, Commun Nonlinear Sci Numer Simulat. 12 (2007) 760–775.

[20] S. Nadeem, Noreen Sher Akbar, M. Y. Malik, Exact and numerical solutions of a micropolar fluid in a vertical annulus, Wiley InterScience, DOI 10.1002/num.20517.

[21] D. Srinivasacharya, J. V. R. Murthy, D. Venugopalam, Unsteady stokes flow of micropolar fluid between two parallel porous plates, Int. J. Engag. Sci. 39 (2001) 1557-1563.

[22] G. Lukaszewicz, Micropolar fluids-theory and applications, Birkhauer, Basel, (1999).

[23] R. Nazar and N. Amin, Free convection boundary layer on an isothermal sphere in a micropolar fluid, Int Comm Heat Mass Tran, 29 (2002) 377-386.

[24] R. Nazara, N. Amina, T. Gro anb and I. Popb,Free convection boundary layer on a sphere with constant surface heat flux in a micropolar fluid, Int Comm Heat Mass Tran, 29 (2002) 1129-1138.

[25] Emad M. Abo-Eldahab, Mohamed A. El Aziz, Flow and heat transfer in a micropolar fluid past a stretching surface embedded in a non-Darcian porous medium with uniform free stream, Appl Math and Comp 162 (2005) 881–899.

[26] S. Nadeem, M. Ali, Analytical solutions for pipe flow of a fourth grade fluid with Reynold and Vogel's models of viscosities, Commun Nonlinear Sci Numer Simulat. 14 (2009) 2073–2090.

[27] S. Nadeem, M. Awais,Thin film flow of an unsteady shrinking sheet through porous medium with variable viscosity, Phy Lett A 372 (2008) 4965–4972.

[28] S. Nadeem, Noreen Sher Akbar, Influence of heat transfer on a peristaltic flow of Johnson Segalman fluid in a non uniform tube, Int Comm Heat Mass Tran 36 (2009) 1050–1059.

[29] S. Nadeem, Anwar Hussain, Majid Khan, HAM solutions for boundary layer flow in the region of the stagnation point towards a stretching sheet, Commun Nonlinear Sci Numer Simulat. 15 (2010) 475–481.

[30] S Liao. A kind of approximate solution technique which does not depend upon small parameters- II. An application in fluid mechanics. Int. J. Non-Linear Mecha, 32 (1997) 815-822.

[31] S. J. Liao, Beyond perturbation: introduction to the homotopy analysis method, Chapman & Hall/CRC Press, Boca Raton (2003).

[32] S. J. Liao, On the homotopy analysis method for nonlinear problems, Appl Math Comput 147/2 (2004) 499–513.

[33] S. Abbasbandy, Homotopy analysis method for the Kawahara equation, Nonlinear Analysis: Real World App. 11 (2010) 307 312.

[34] S. Abbasbandy, Homotopy analysis method for heat radiation equations, Int Comm Heat Mass Tran 34 (2007) 380–387.

[35] S. Abbasbandy, Soliton solutions for the Fitzhugh-Nagumo equation with the homotopy analysis method Appl.Math Mod 32 (2008) 2706 2714.

[36] S. J. Liao, Notes on the homotopy analysis method: some definitions and theorems. commun Nonlinear Sci. Numer. Simulat 14 (2009) 983-997.